Fast Crystal Scintillators for GHz Hard X-Ray Imaging

Chen Hu, Fan Yang, Liyuan Zhang, Ren-Yuan Zhu,

California Institute of Technology

Aiping Chen, Zhehui Wang,

Los Alamos National Laboratory

Lei Ying and Zongfu Yu

University of Wisconsin

September 13, 2018

Presentation in the ULITIMA 2018 Conference at ANL

GHz Hard X-Ray Imaging

High-Energy and Ultrafast X-Ray Imaging Technologies and Applications

Organizers: Peter Denes, Sol Gruner, Michael Stevens & Zhehui (Jeff) Wang[1]
*(**Location/Time**: Santa Fe, NM, USA /Aug 2-3, 2016)*

The goals of this workshop are to gather the leading experts in the related fields, to prioritize tasks for ultrafast hard X-ray imaging detector technology development and applications in the next 5 to 10 years, see Table 1, and to establish the foundations for near-term R&D collaborations.

Table I. High-energy photon imagers for MaRIE XFEL

Performance	Type I imager	Type II imager
X-ray energy	30 keV	42-126 keV
Frame-rate/inter-frame time	0.5 GHz/2 ns	3 GHz / 300 ps
Number of frames	10	10 - 30
X-ray detection efficiency	above 50%	above 80%
Pixel size/pitch	≤ 300 μm	< 300 μm
Dynamic range	10^3 X-ray photons	≥ 10^4 X-ray photons
Pixel format	64 x 64 (scalable to 1 Mpix)	1 Mpix

2 ns and 300 ps inter-frame time requires very fast scintillator and sensor

Why Crystal Scintillator?

- Detection efficiency for hard X-ray requires bulk detector.
- Scintillation light provides fast signal.
- Pixelized crystal detector is a standard for medical industry.
- A detector concept:
  - Pixelized fast scintillator screen;
  - Pixelized fast photodetector;
  - Fast electronics readout.
- Challenges:

  Ultra-fast crystals, photodetectors and readout.

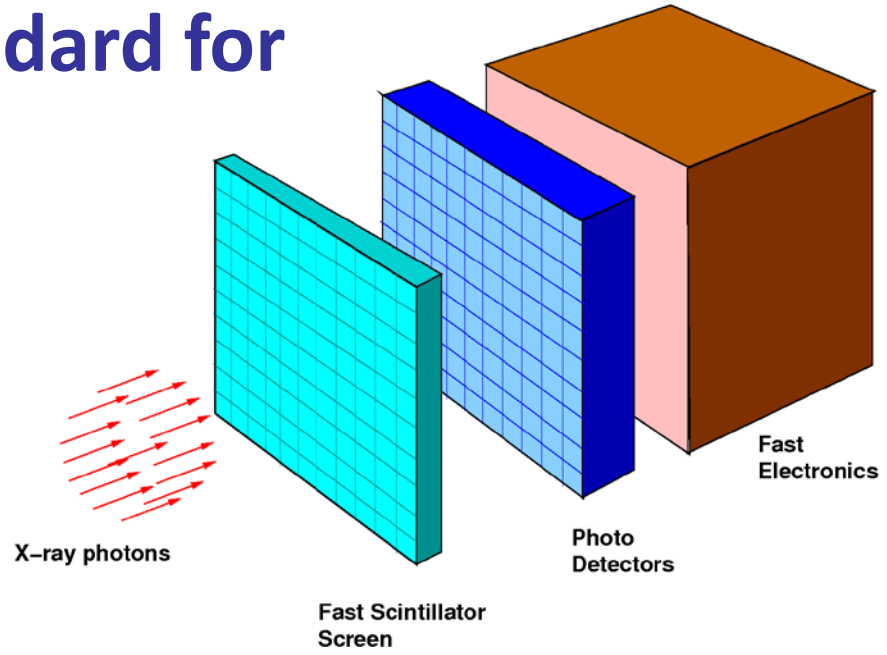

Pixelized Crystal Detectors

Crystal panels of 300 μ pitch may be fabricated by classical mechanical processing

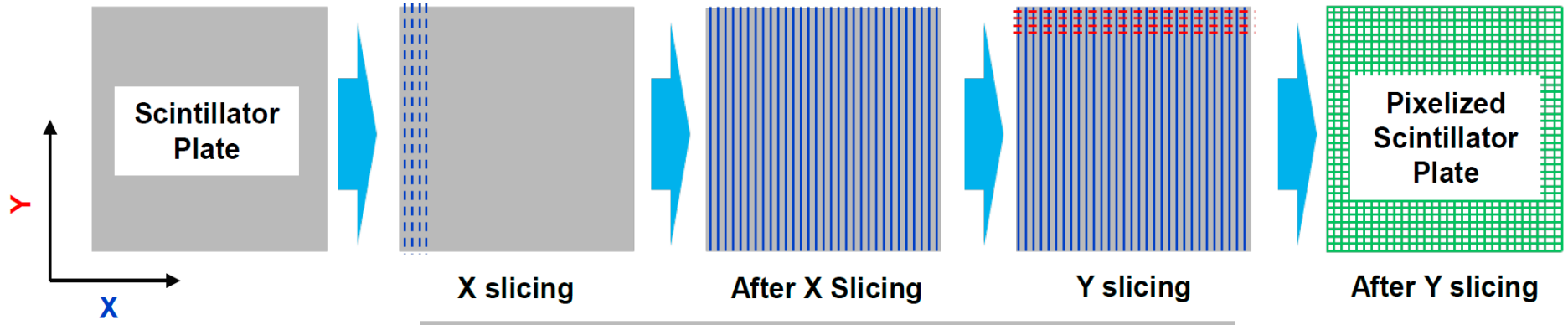

A Schematic showing pixelized scintillator plate processing

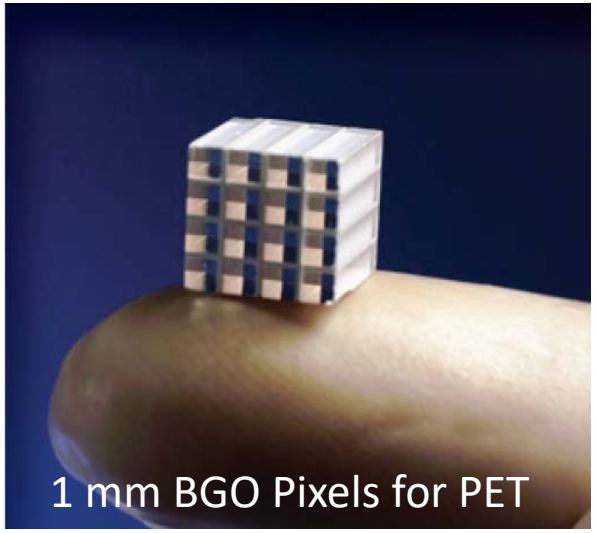

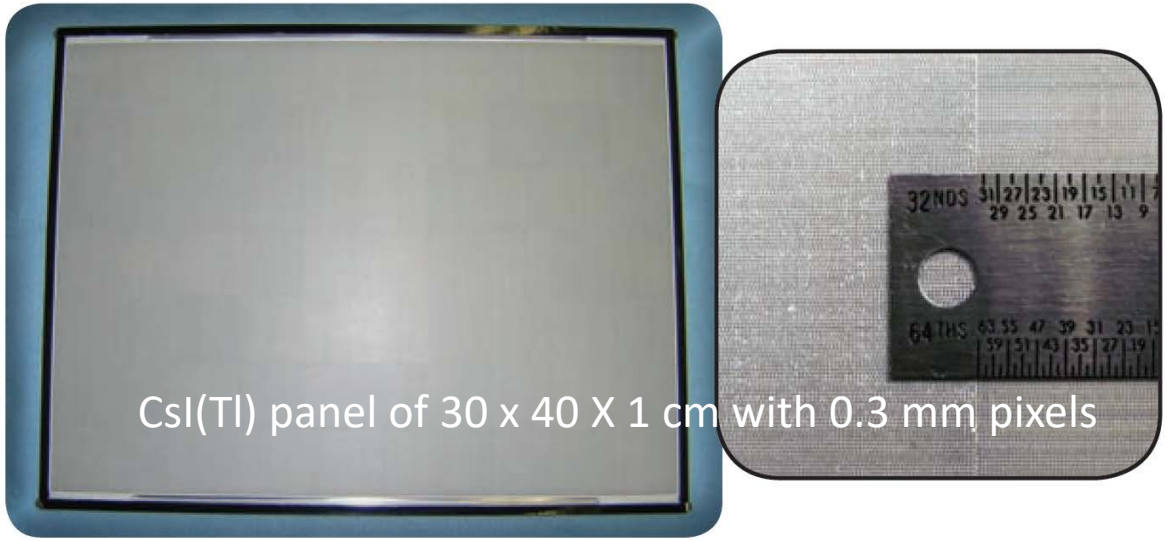

Laser slicing and not pixelized may provide better coverage

Candidate Scintillators for Marie

	LYSO (:Ce)	YSO:Ce	ZnO:Ga	BaF_2	BaF_2:Y	YAP:Ce	YAP:Yb	YAG:Yb	LuAG:Ce	$LaBr_3$ (:Ce)
Density (g/cm^3)	7.4	4.44	5.67	4.89	4.89	5.35	5.35	4.56	6.76	5.29
Melting points (°C)	2050	2070	1975	1280	1280	1870	1870	1940	2060	783
X_0 (cm)	1.14	3.10	2.51	2.03	2.03	2.77	2.77	3.53	1.45	1.88
R_M (cm)	2.07	2.93	2.28	3.1	3.1	2.4	2.4	2.76	2.15	2.85
λ_I (cm)	20.9	27.8	22.2	30.7	30.7	22.4	22.4	25.2	20.6	30.4
Z_{eff}	64.8	33.3	27.7	51.6	51.6	31.9	31.9	30	60.3	45.6
dE/dX (MeV/cm)	9.55	6.57	8.42	6.52	6.52	8.05	8.05	7.01	9.22	6.90
λ_{peak} [a] (nm)	420	420	389	300 220	300 220	370	350	350	520	360
Refractive Index[b]	1.82	1.78	2.1	1.50	1.50	1.96	1.96	1.87	1.84	1.9
Normalized Light Yield[a,c]	100	80	6.6[e]	42 4.8	1.7 4.8	9 32	0.19[e]	0.36[e]	35[f] 48[f]	153
Total Light yield (ph/MeV)	30,000	24,000	2,000[e]	13,000	2,000	12,000	57[e]	110[e]	25,000[f]	46,000
Decay time[a] (ns)	40	75	<1	600 0.6	600 0.6	191 25	1.5	4	981[f] 64[f]	20
Light Yield in 1st ns (photons/MeV)	740	318	610[e]	1200	1200	391	28[e]	24[e]	240	2,200
40 keV Att. Length (1/e, mm)	0.185	0.334	0.407	0.106	0.106	0.314	0.314	0.439	0.251	0.131

[1] Spurrier, et al., *IEEE T. Nucl. Sci.* 2008,55 (3): 1178-1182.

a. Top line: slow component, bottom line: fast component;
b. At the wavelength of the emission maximum;
c. Excited by Gamma rays;
d. For 0.4 at% Ca co-doping;
e. Excited by Alpha particles.
f. Ceramic with 0.3 Mg at% co-doping

LYSO and ZnO:Ga Samples

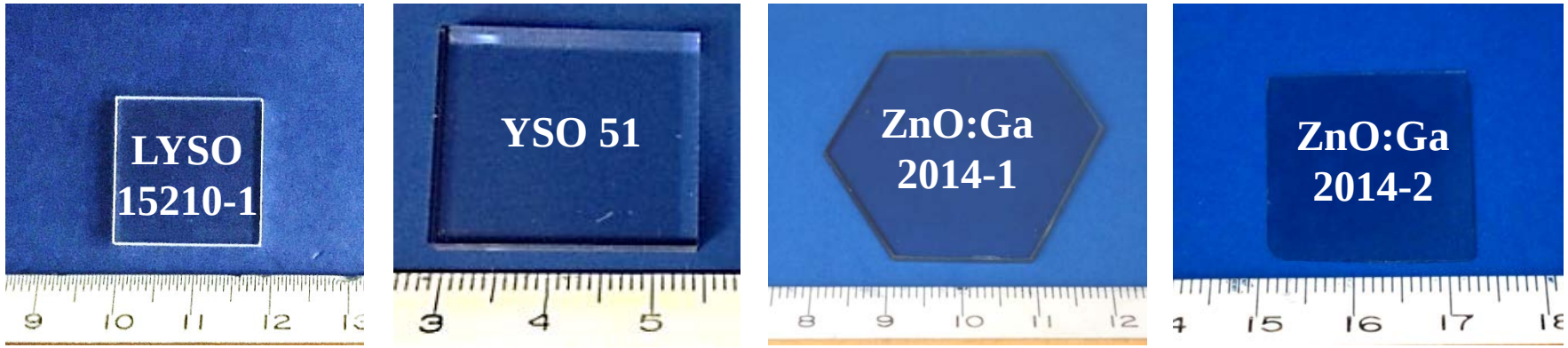

Crystal	Vendor	ID	Dimension (mm^3)
LYSO:Ce	SIC	150210-1	19x19×2
YSO:Ce	SIC	51	25×25×5
ZnO:Ga	FJIRSM	2014-1	33×30×2
ZnO:Ga	FJIRSM	2014-2	22×22×0.3

Experiments

- Properties measured at room temperature : PL & Decay, Transmittance, PHS, LO & Decay kinetics

SIC LYSO:Ce-150210-1

✓ High LO, good transmittance and ER, short decay time

× Decay time too long for X-ray frame rate of a few ns

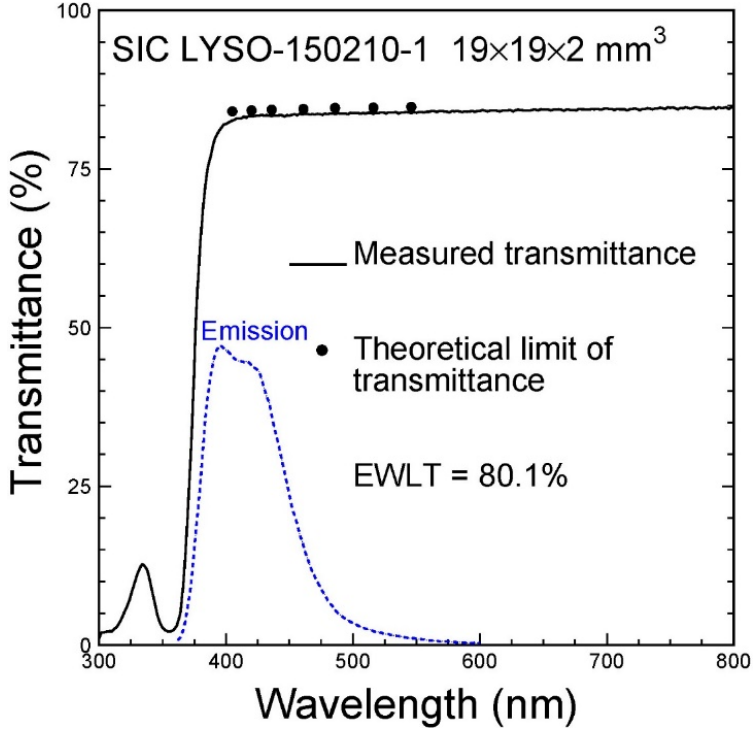

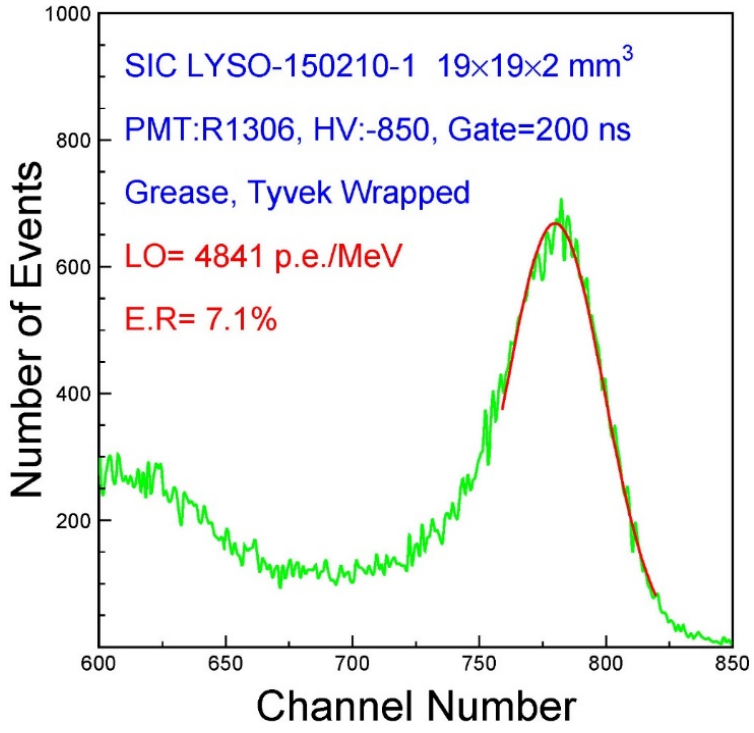

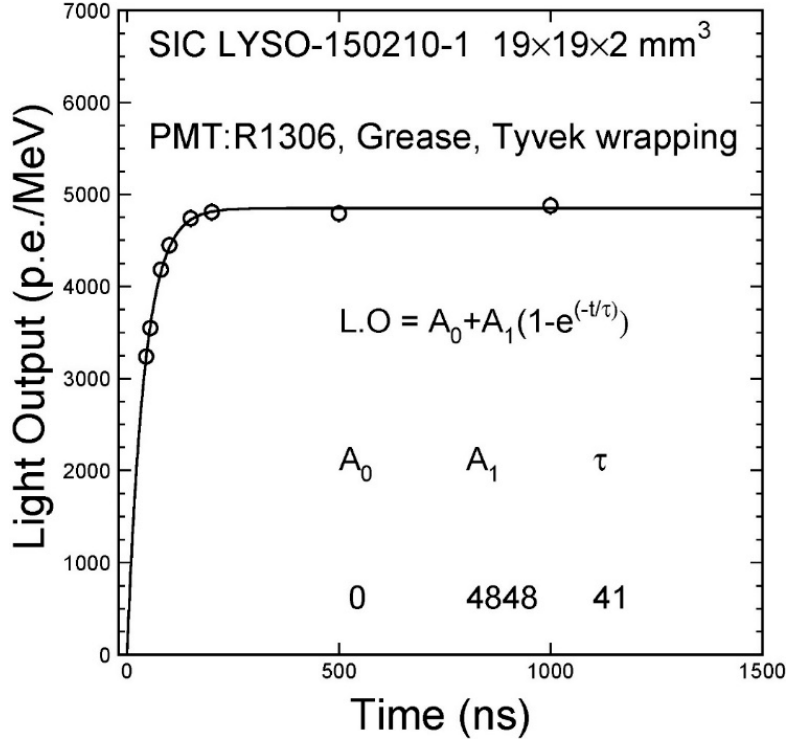

ID	Dimension	EWLT (%)	ER (%)	200 ns LO (p.e./MeV)	Primary Decay Time (ns)
SIC LYSO-150210-1	19×19×2	80.1	7.1	4841	41

SIC YSO:Ce-51 (in LANL)

✓ Good LO, transmittance, ER, and short decay time

× All these performance are inferior to LYSO:Ce

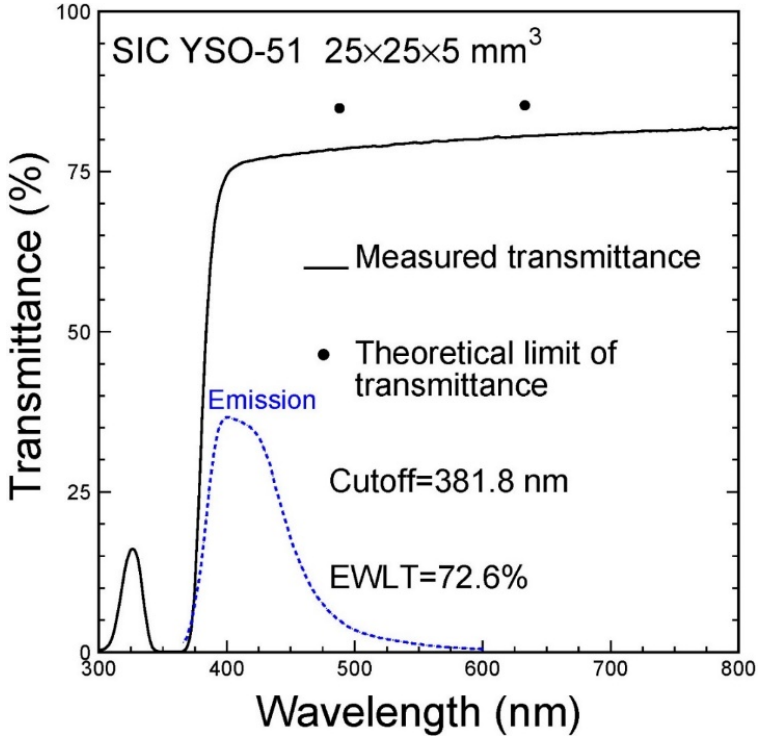

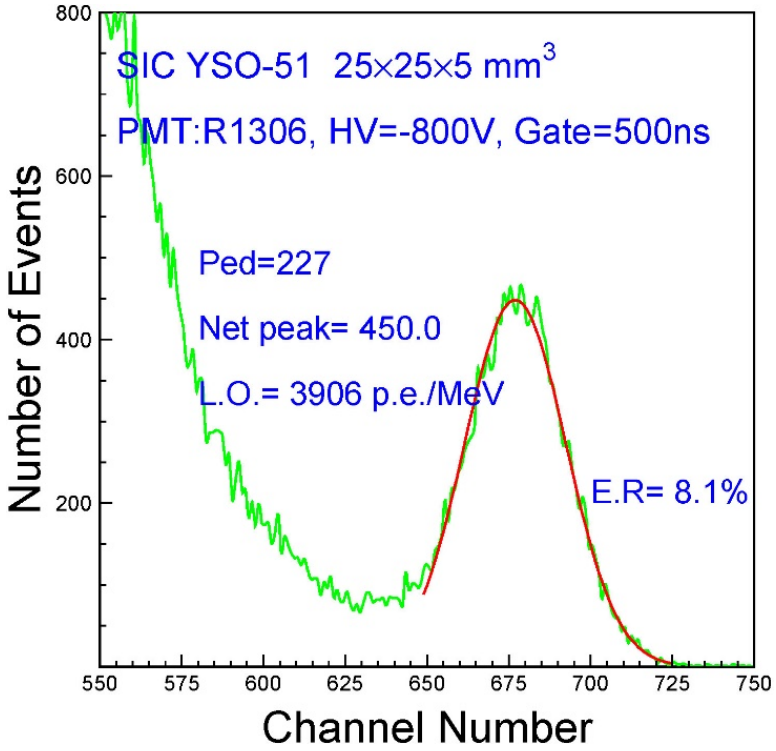

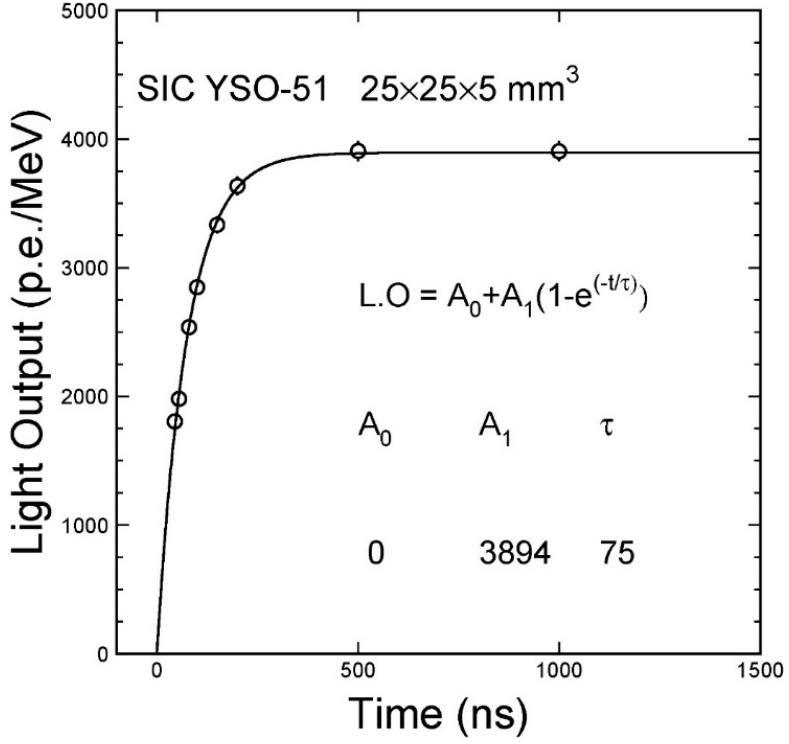

ID	Dimension	EWLT (%)	ER (%)	500 ns LO (p.e./MeV)	Primary Decay Time (ns)
SIC YSO-51	25×25×5	72.6	8.1	3906	75

FJIRSM ZnO:Ga-2014-1

✓ Very short decay time

× Low EWLT and LO due to severe self absorption

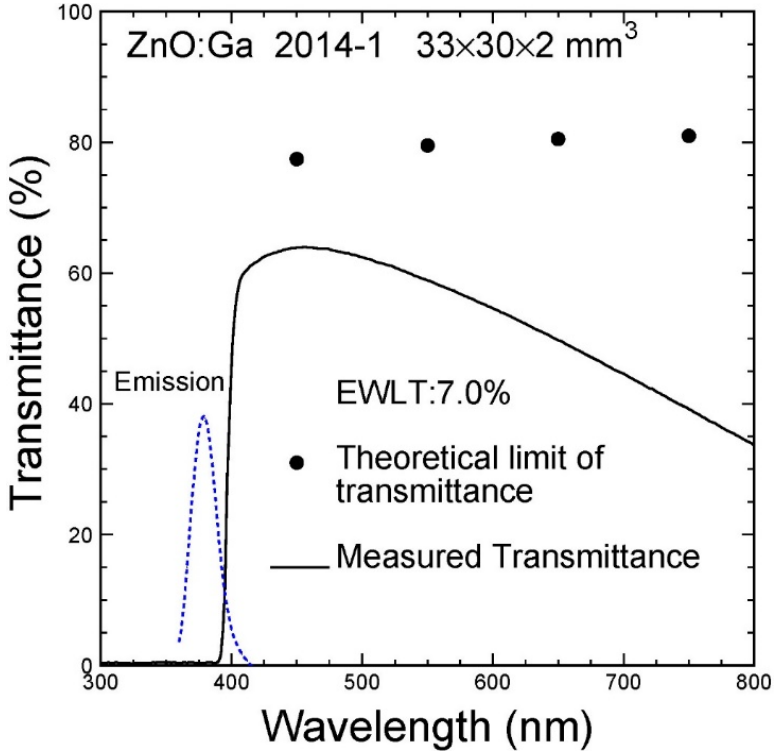

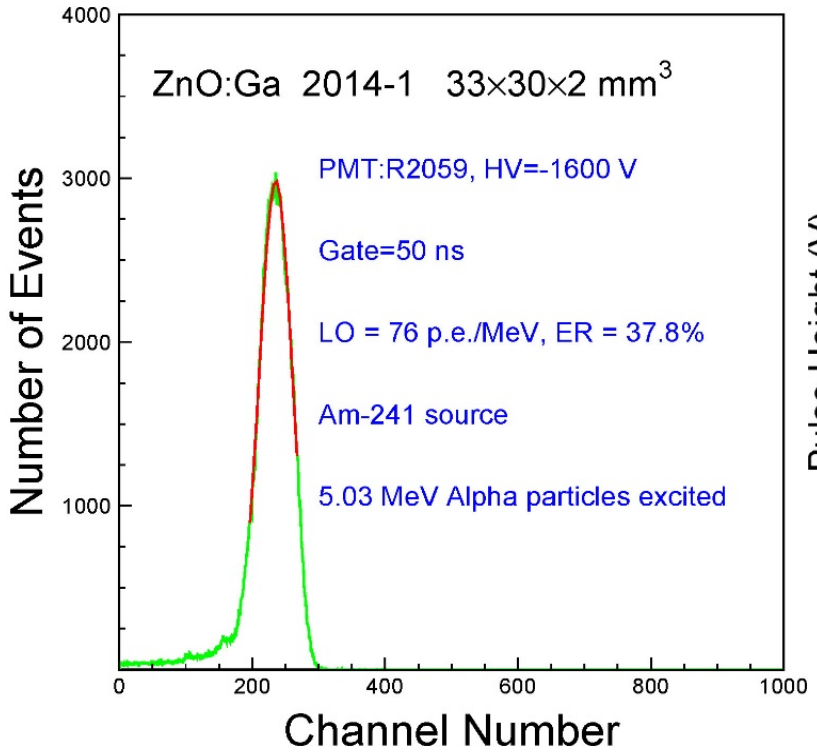

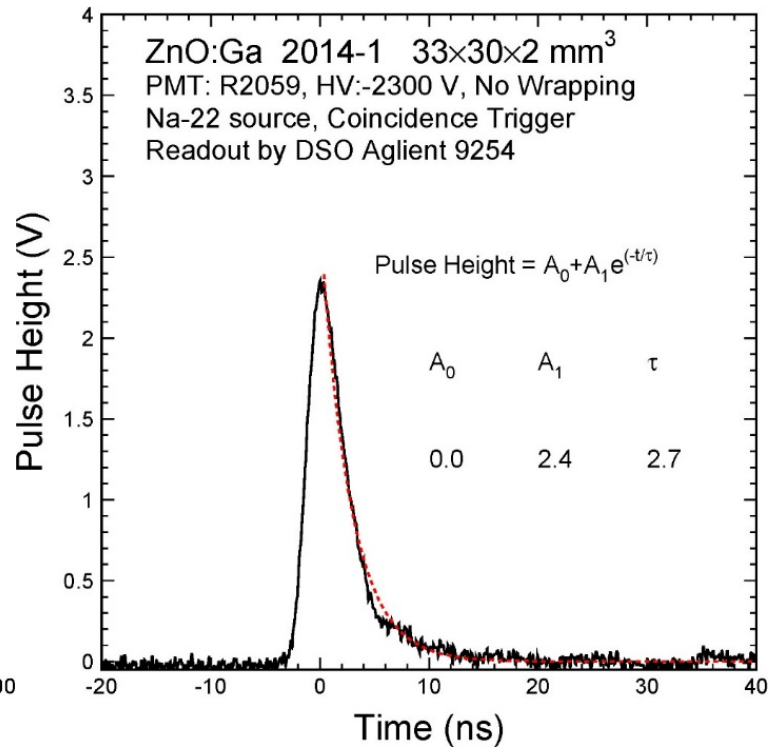

ID	Dimension	EWLT (%)	ER (%)	50 ns LO (p.e./MeV)	Primary Decay Time (ns)
FJIRSM ZnO:Ga-2014-1	33×30×2	7.0	37.8	76 (α)	2.7

FJIRSM ZnO:Ga-2014-2

× Reduced self absorption due to 0.3 mm thickness

× May pursue QD, NP or thin film based solution

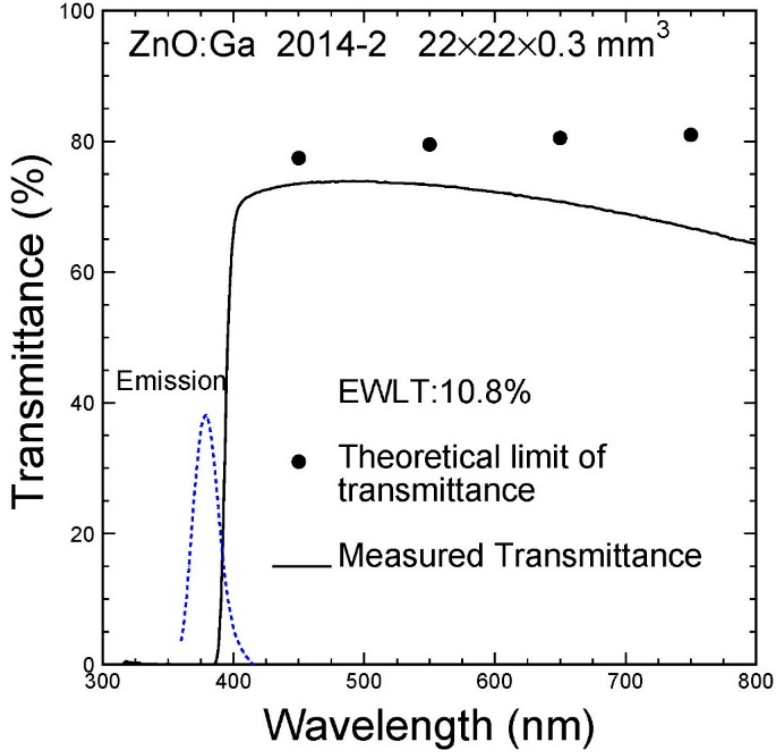

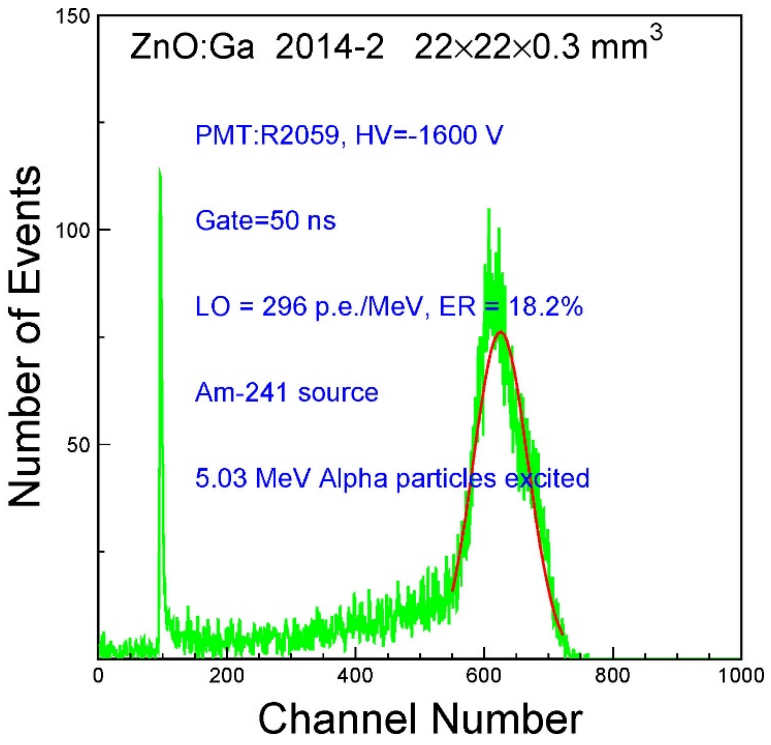

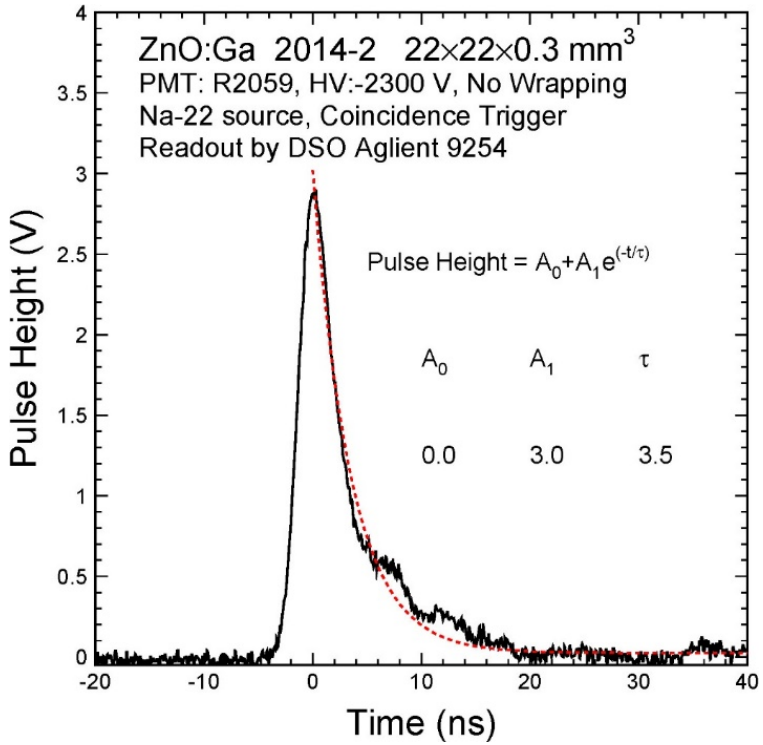

ID	Dimension	EWLT (%)	ER (%)	50 ns LO (p.e./MeV)	Primary Decay Time (ns)
FJIRSM ZnO:Ga-2014-2	22×22×0.3	10.8	18.2	296 (α)	3.5

BaF_2 and Other Samples

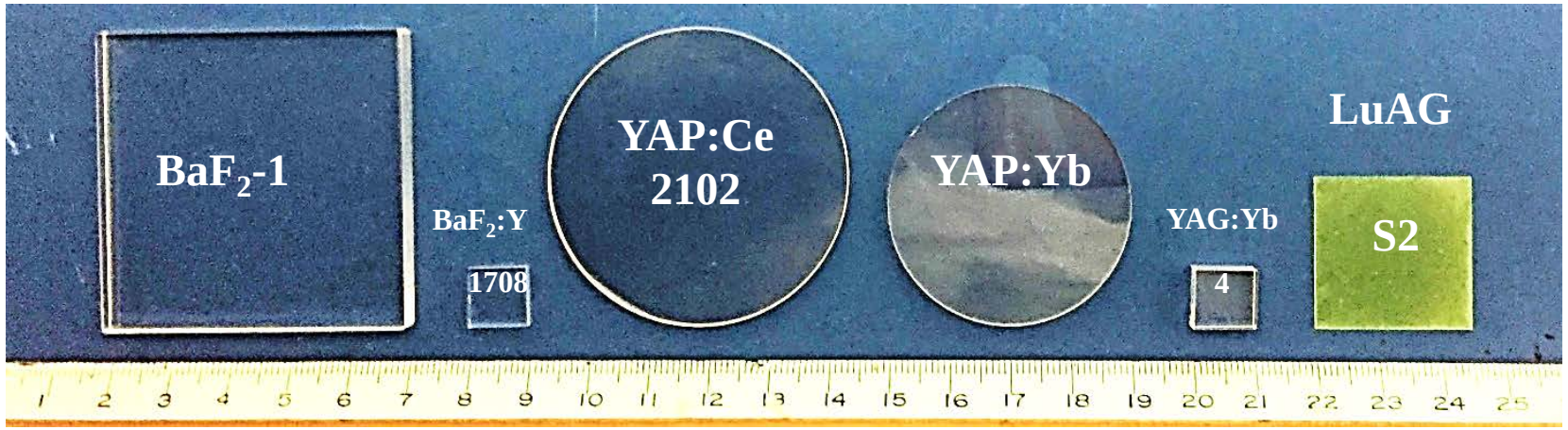

Crystal	Vendor	ID	Dimension (mm^3)
BaF_2	SIC	1	50×50×5
BaF_2:Y	BGRI	1708	10×10×2
YAP:Ce	Dongjun	2102	Φ50×2
YAP:Yb	Dongjun	2-2	Φ40×2
YAG:Yb	Dongjun	4	10×10×5
LuAG:Ce	SIC	S2	25×25×0.4

Experiments

- Properties measured at room temperature : PL & Decay, Transmittance, PHS, LO & Decay kinetics

SIC BaF_2-1

✓ The highest LY in 1st ns among all non-hygroscopic scintillators

× ~600 ns slow component may be suppressed by Y doping

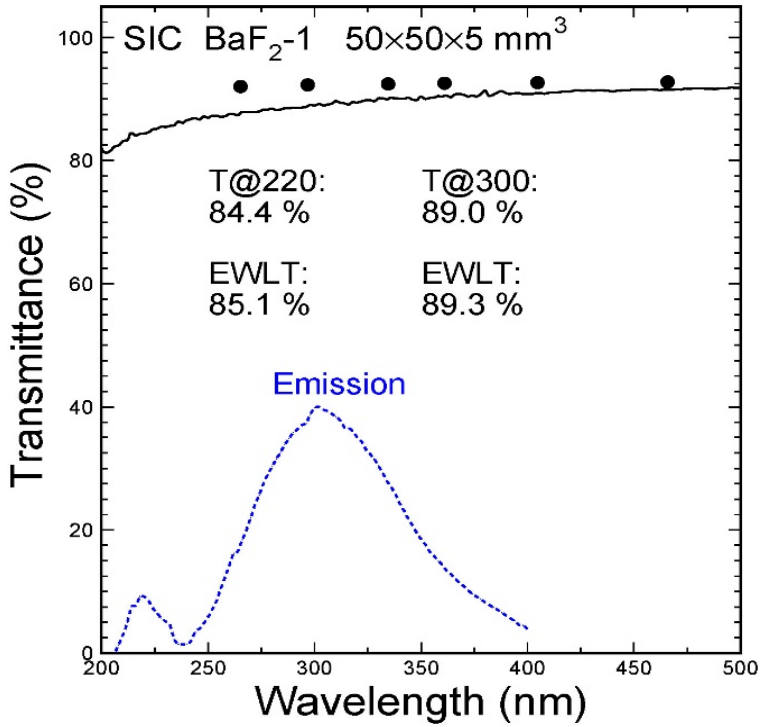

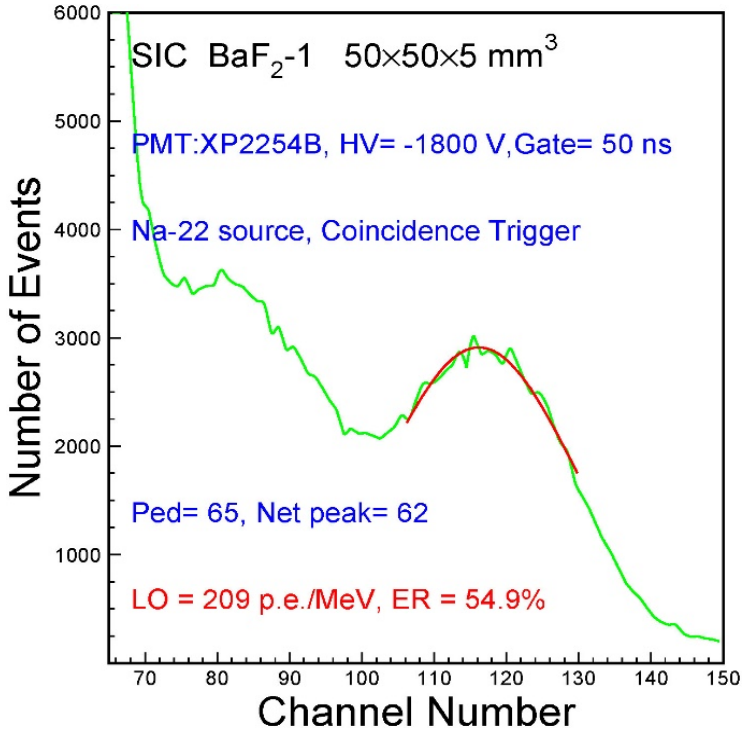

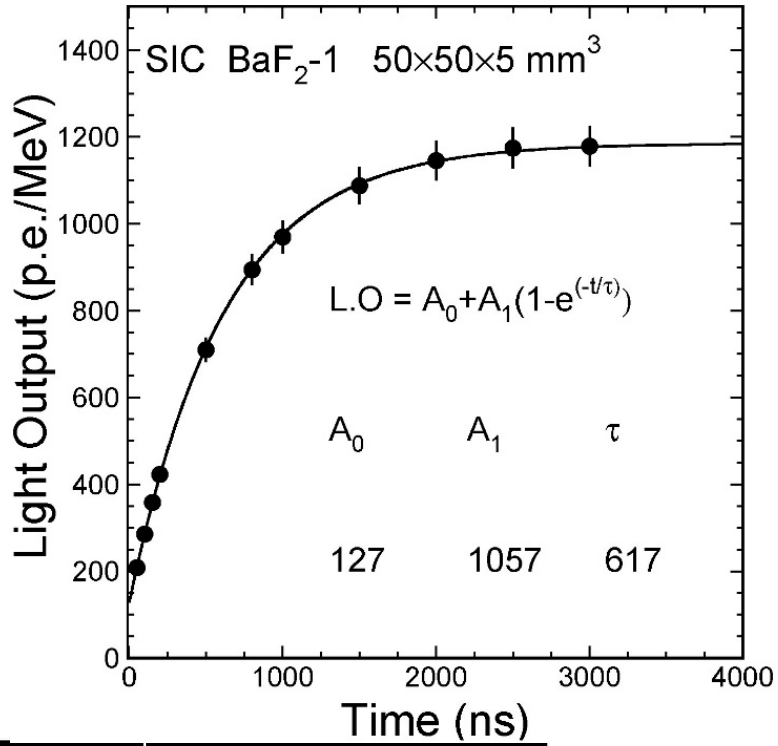

ID	Dimension	EWLT (%)	ER (%)	50 ns LO (p.e./MeV)	Primary Decay Time (ns)
SIC BaF_2-1	50×50×5	85.1	54.9	209	0.6

Yttrium Doping in BaF_2

While the fast component in BaF_2 keeps more or less the same,
The slow component is significantly suppressed by Yttrium doping.

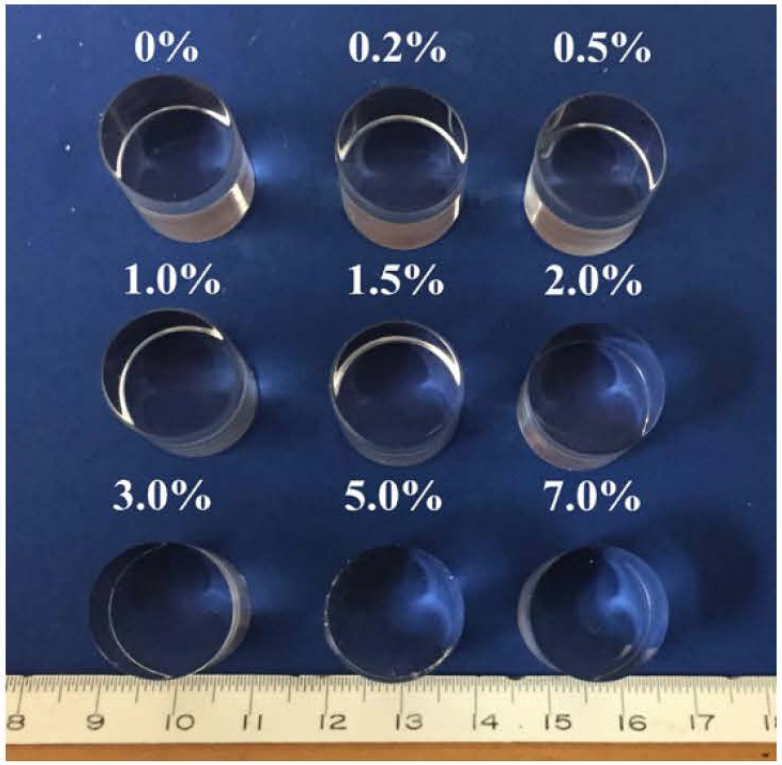

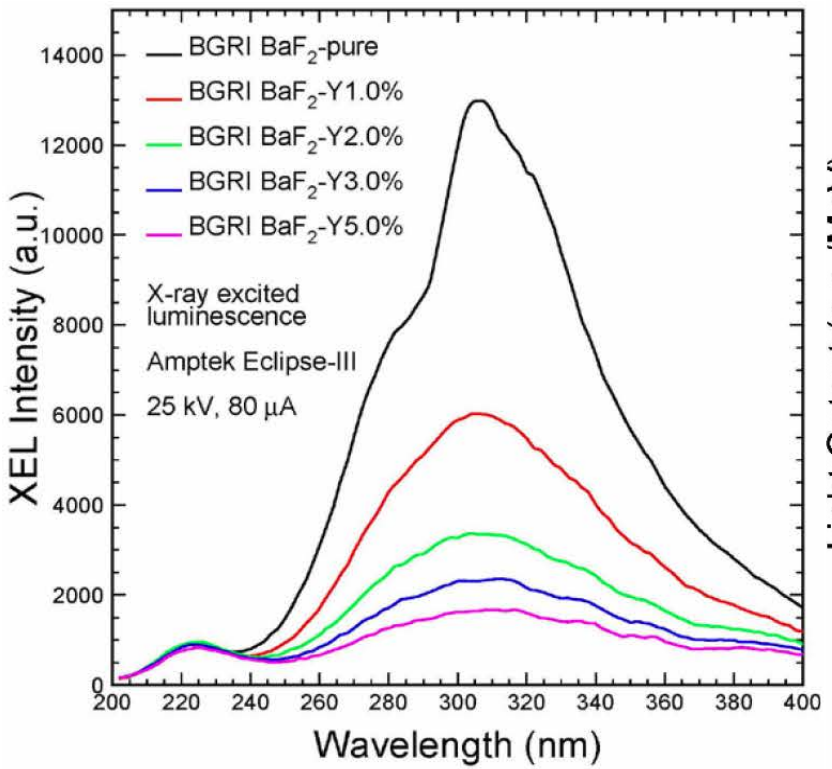

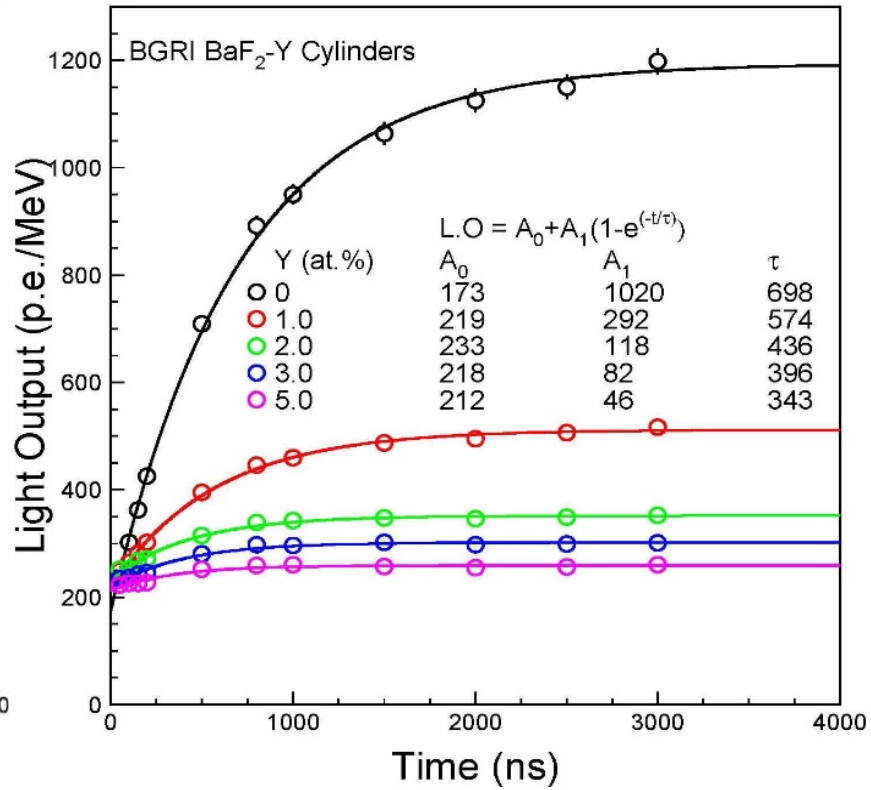

BGRI Y Doped/Undoped BaF_2

Fast/Slow ratio increased from 0.20 to 3.2

Y-doped

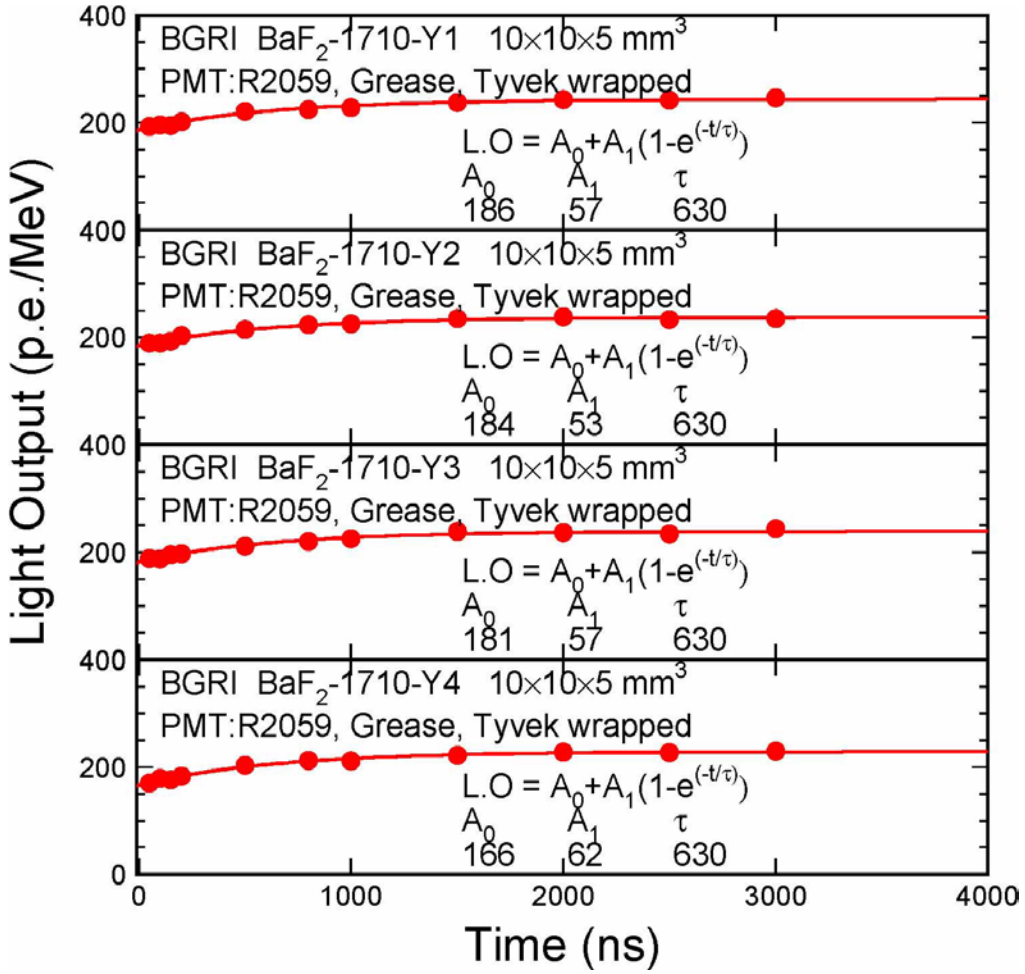

Undoped

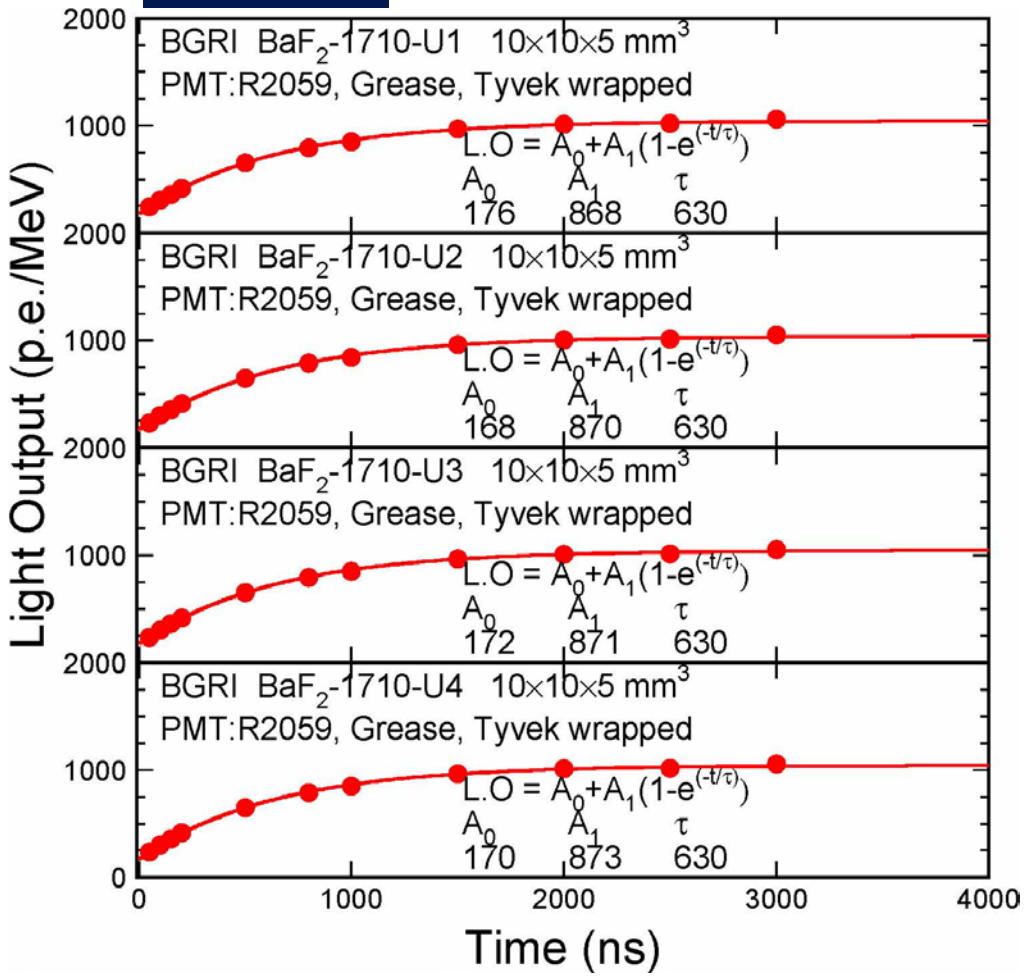

γ-ray induced damage in BaF_2

- BaF_2 crystals of 25 cm long were irradiated by Co-60 at Caltech and JPL.
- 40% fast scintillation light remains after 120 Mrad ionization dose at JPL.

IEEE Trans. Nucl. Sci. NS-63 (2016) 612-619

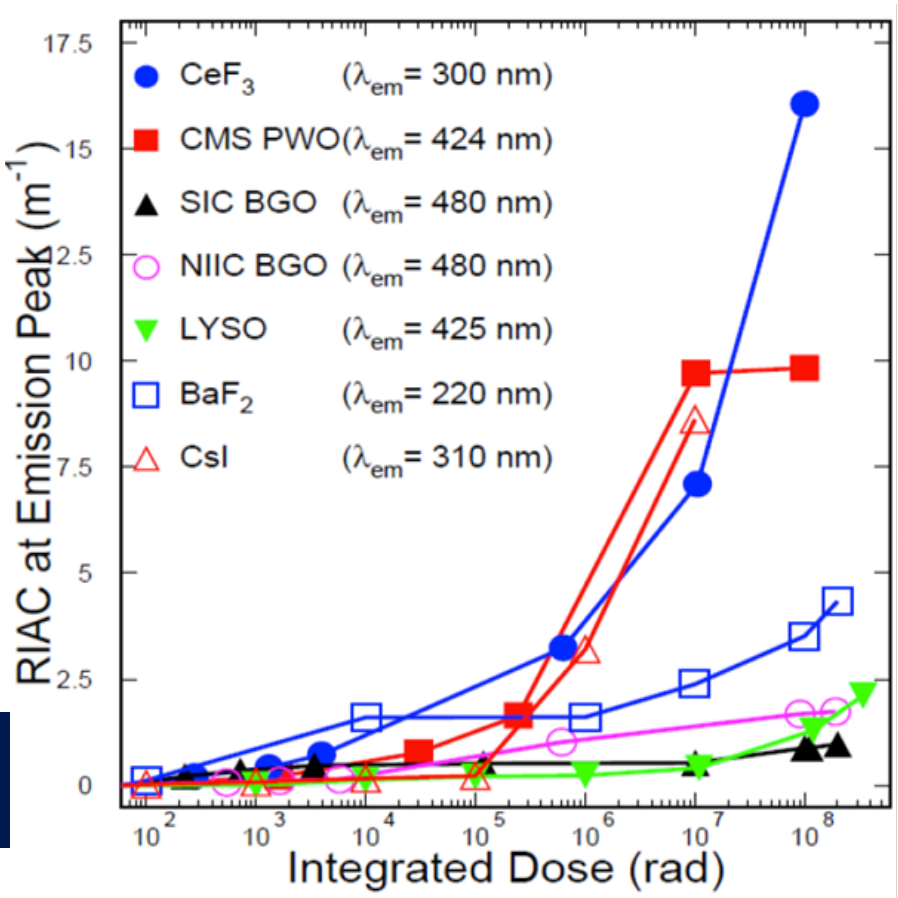

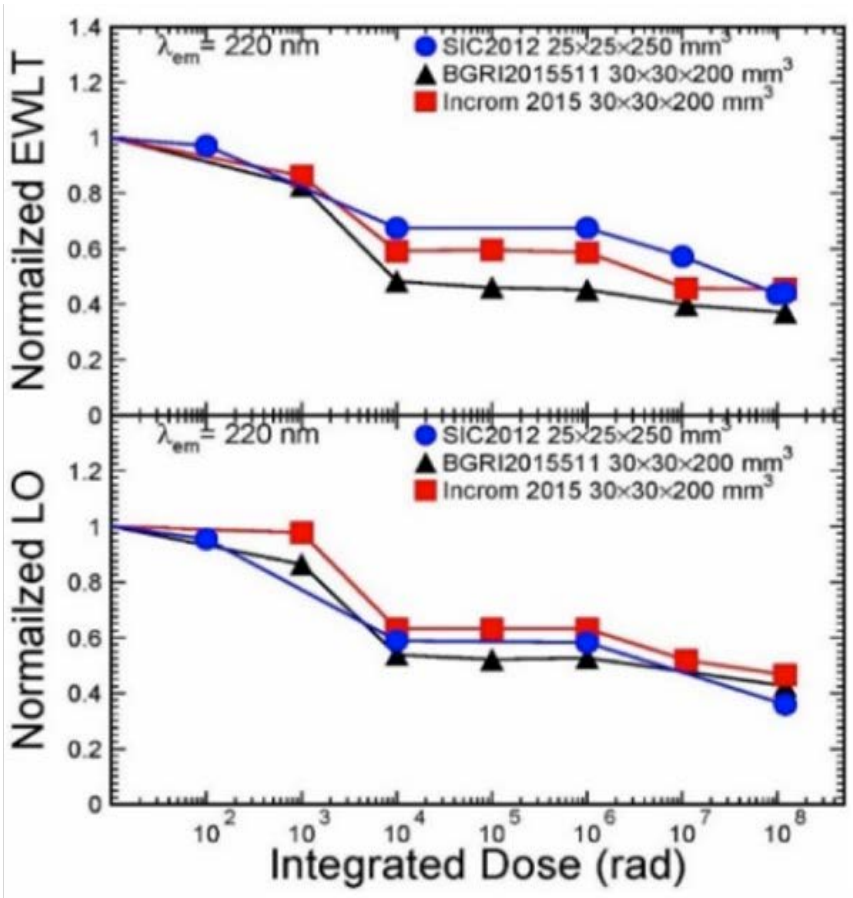

Proton induced damage in BaF_2

- BaF_2 plates of 5 mm thick were irradiated by 800 MeV at LANL in 2016.
- 90% fast scintillation light remains after 10^{15} p/cm^2.

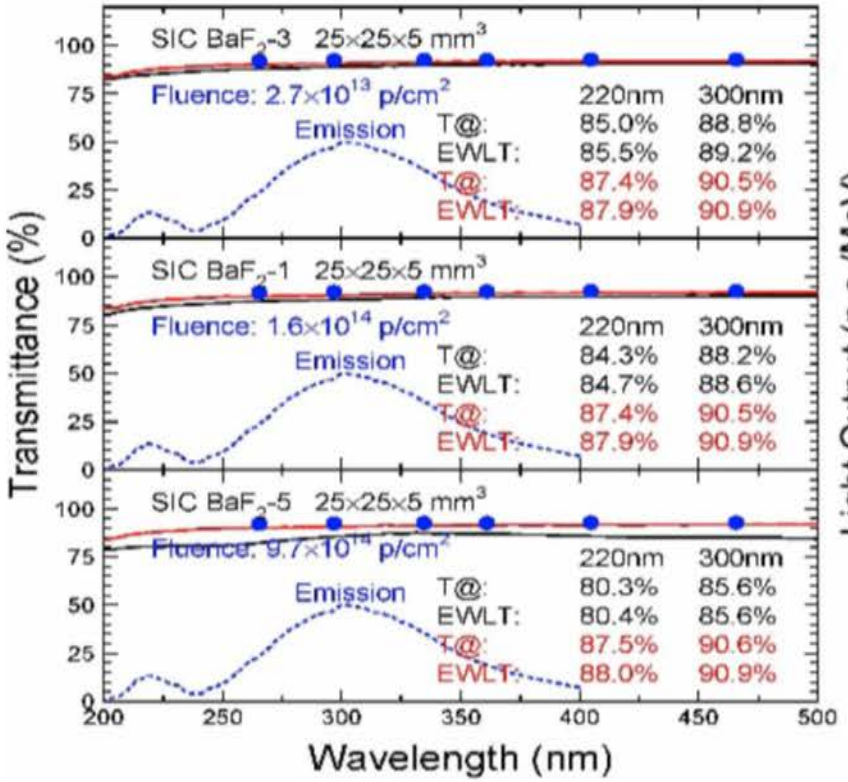

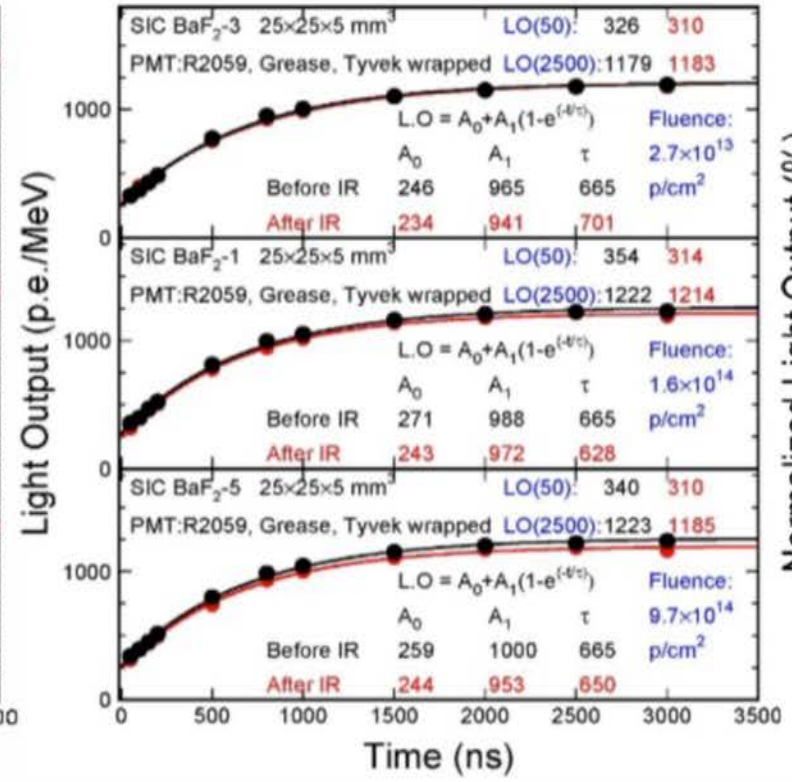

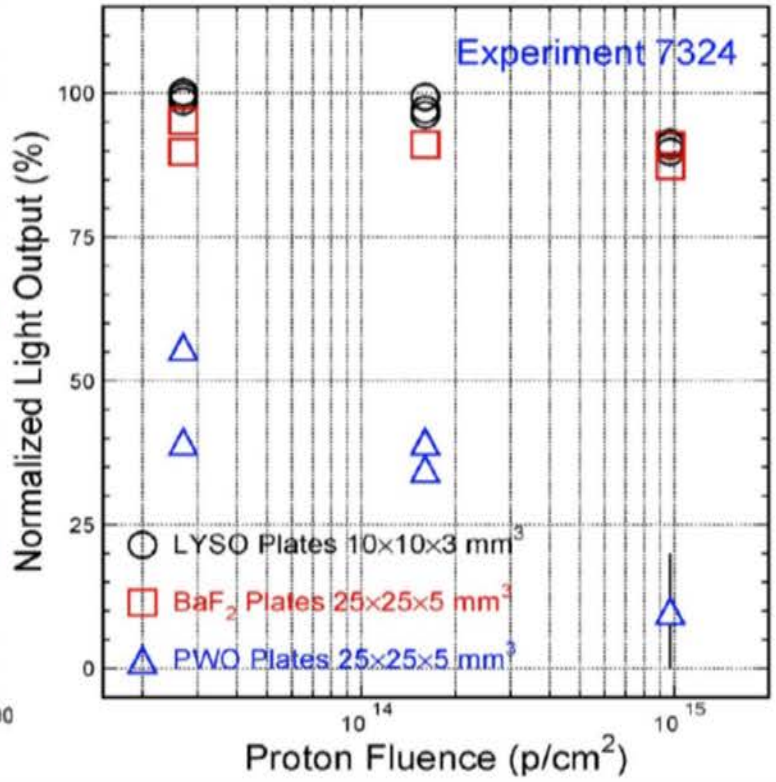

IEEE Trans. Nucl. Sci. NS-65 (2018) 1018-1024

Neutron induced damage in BaF_2

- BaF_2 plates of 5 mm thick were irradiated by neutrons at LANL in 2016.
- 75% fast scintillation light remains after 3×10^{15} n (>1 MeV)/cm^2.

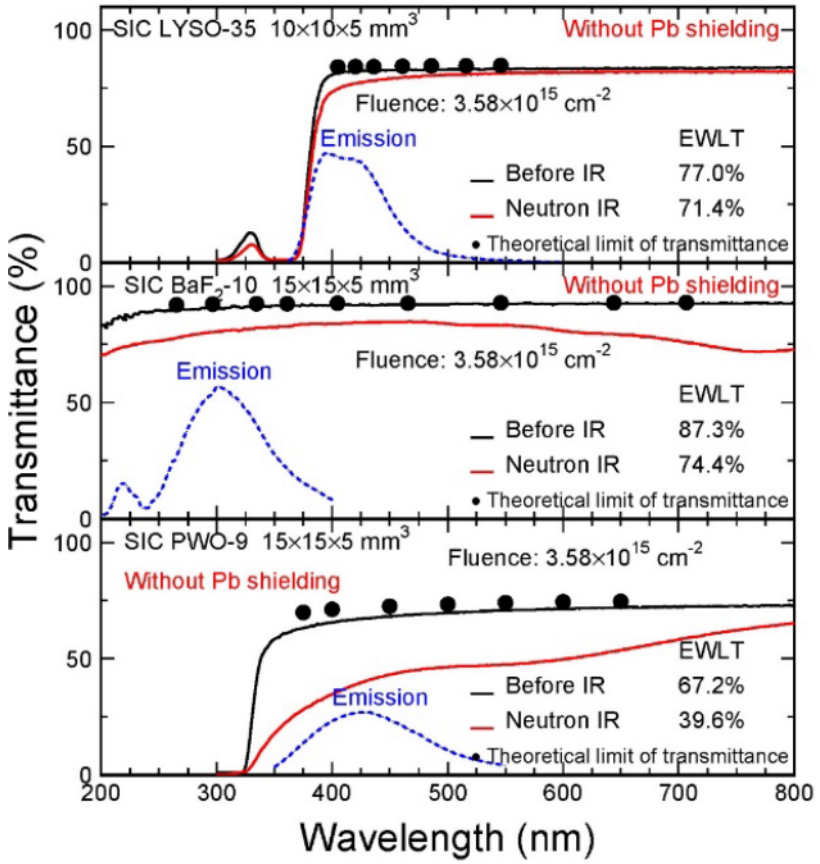

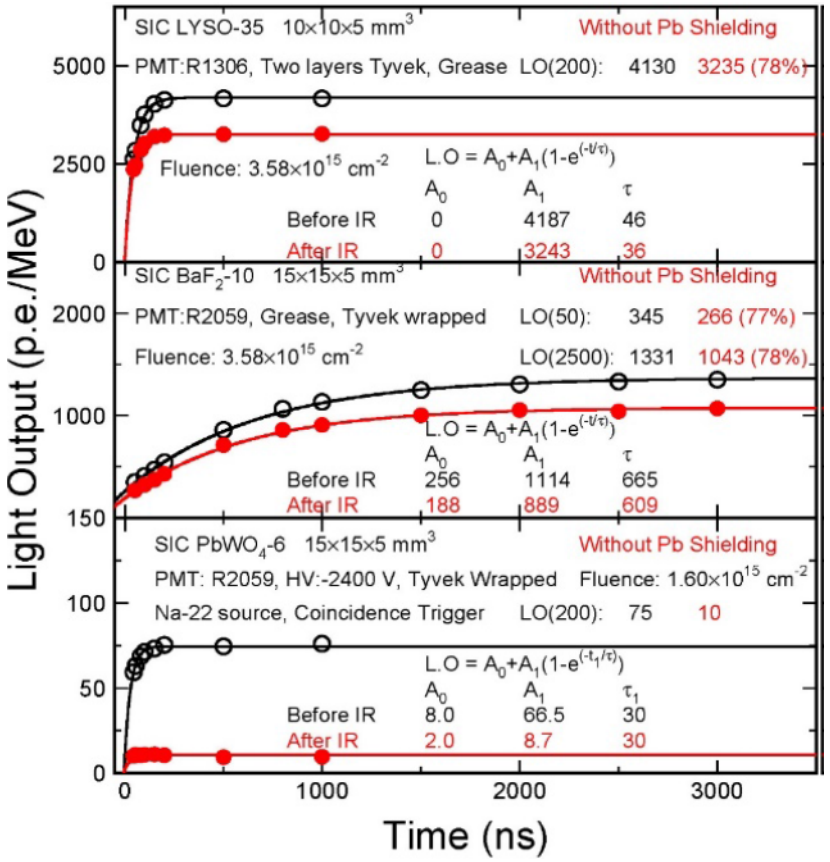

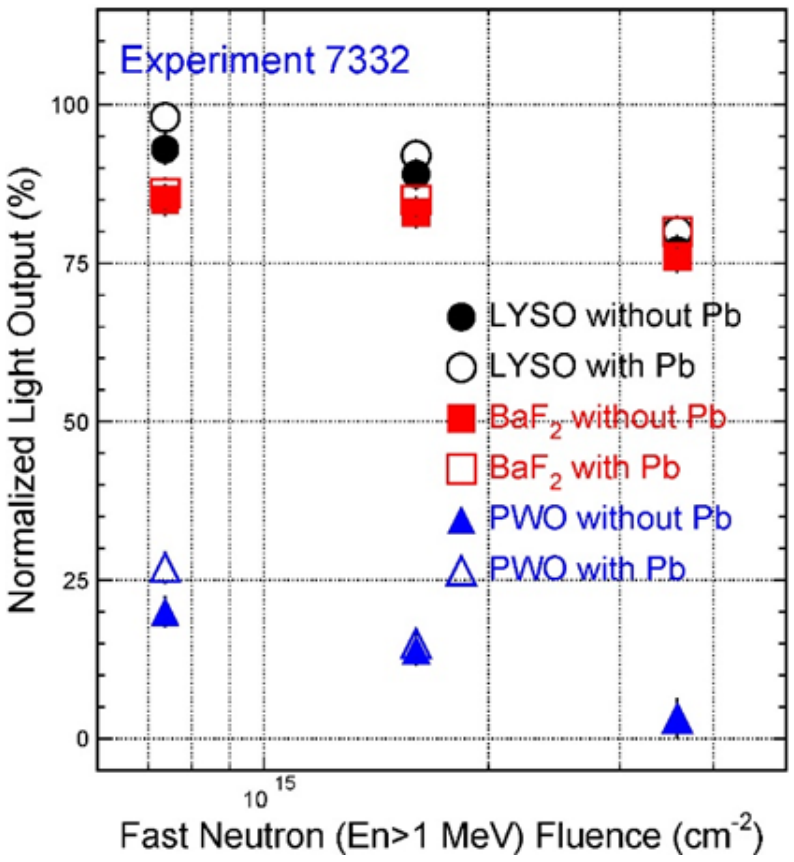

To be published in the proceedings of CALOR2018

DJ YAP:Ce-2102

✓ Adequate LO and ER

× Self absorption and slow component

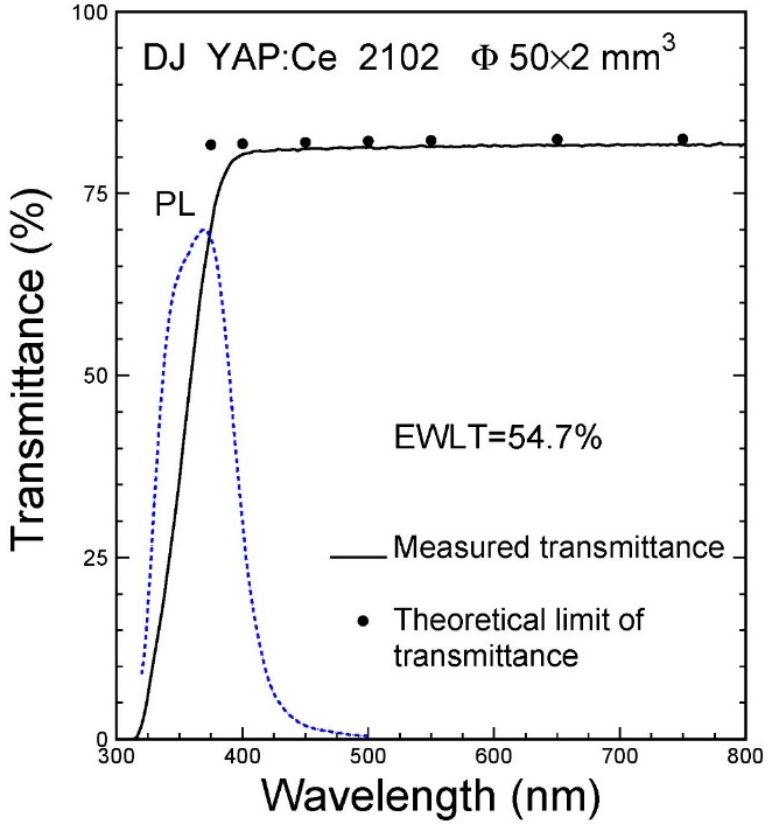

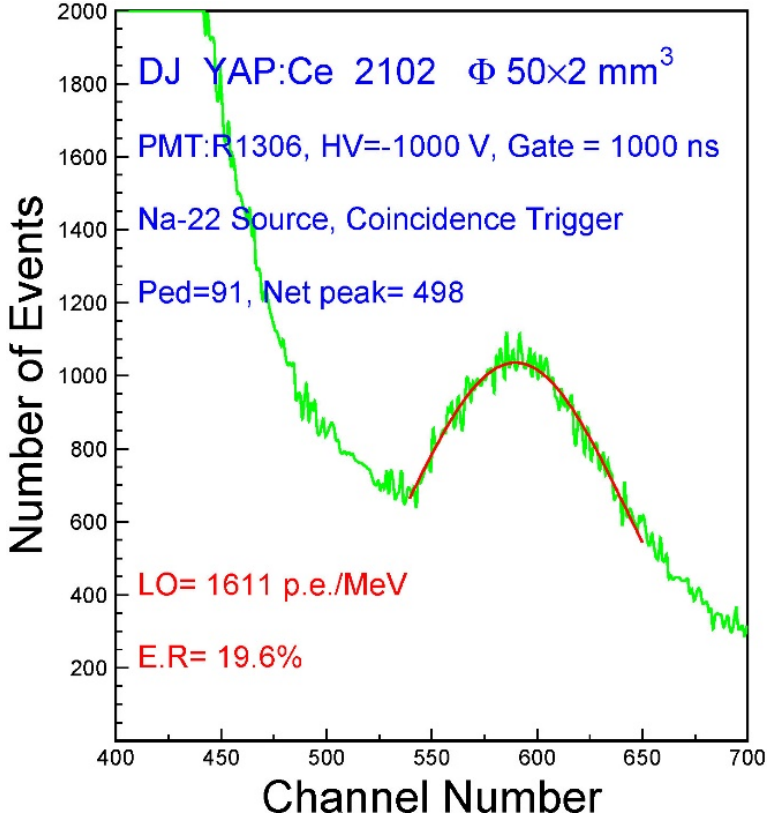

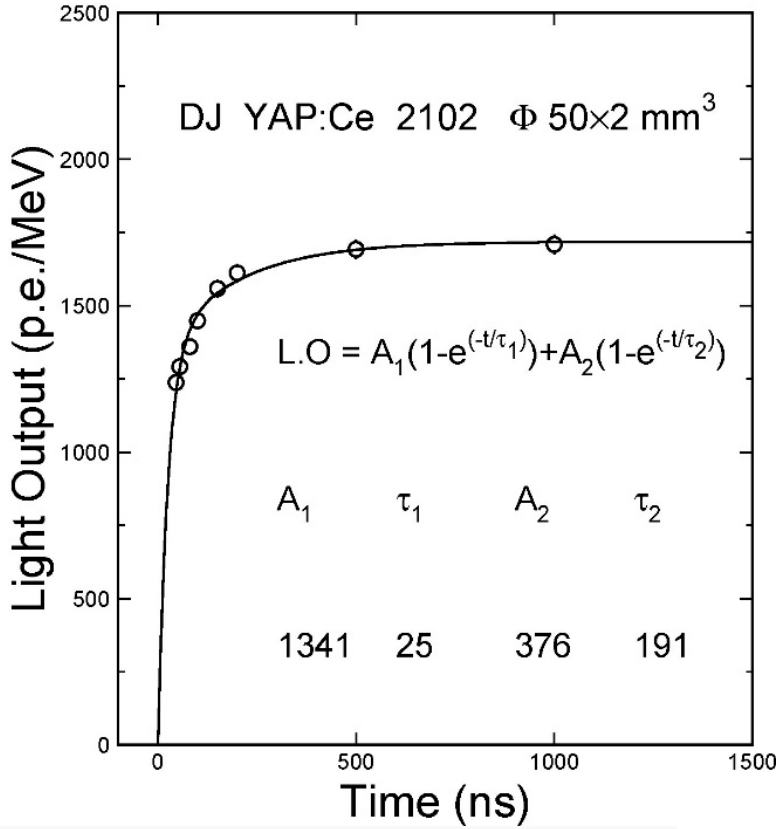

ID	Dimension	EWLT (%)	ER (%)	200 ns LO (p.e./MeV)	Primary Decay Time (ns)
DJ YAP:Ce-2102	Φ50×2	54.7	19.6	1611	25

DJ YAP:Yb-2-2

✓ Very short decay time

× Low LO due to thermal quenching

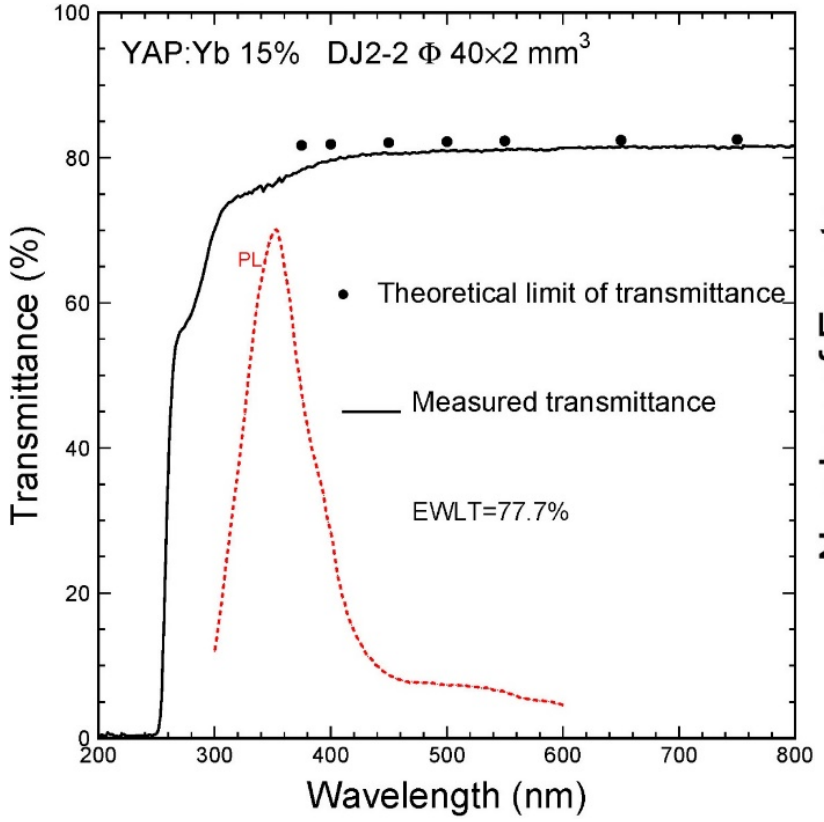

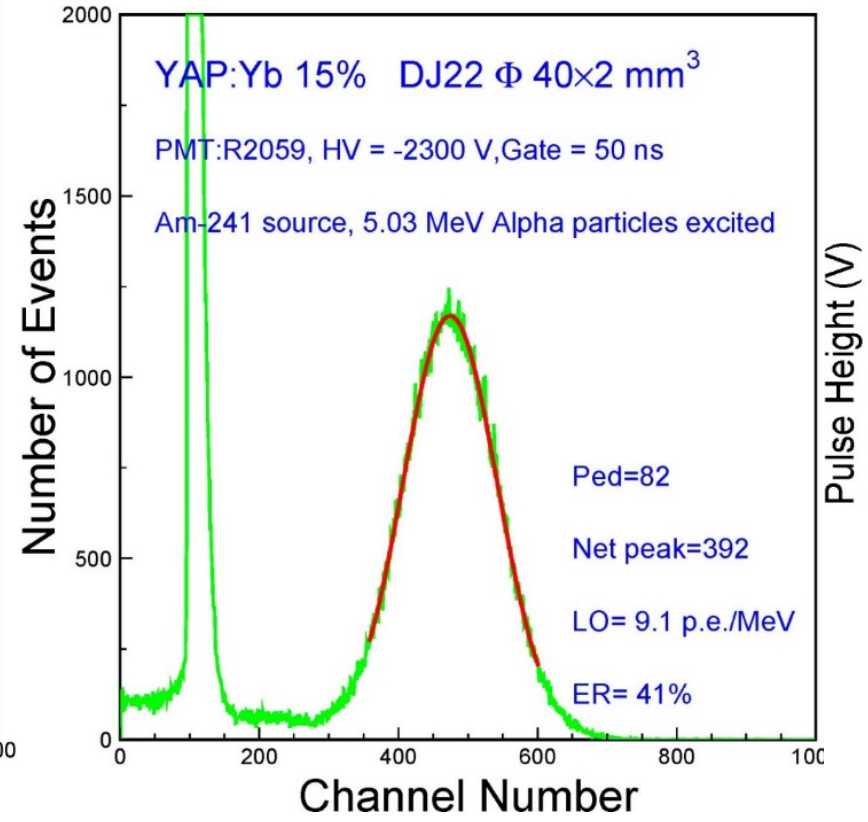

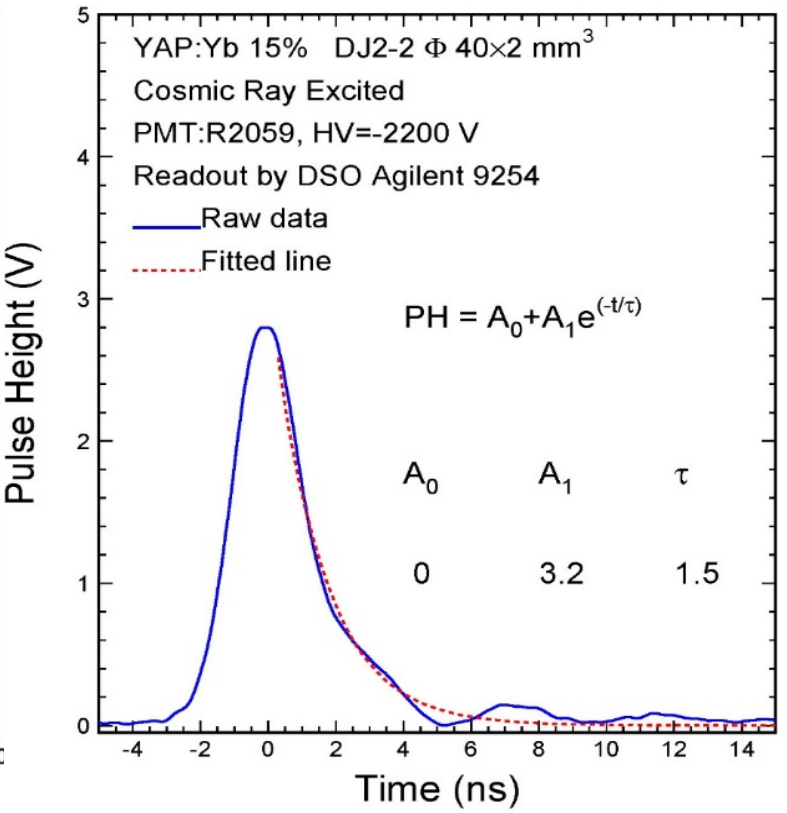

ID	Dimension	EWLT (%)	ER (%)	50 ns LO (p.e./MeV)	Primary Decay Time (ns)
DJ YAP:Yb-2-2	Φ40×2	77.7	41	9.1 (α)	1.5

DJ YAG:Yb-4

✓ Very short decay time and good transmittance

× Low LO due to thermal quenching

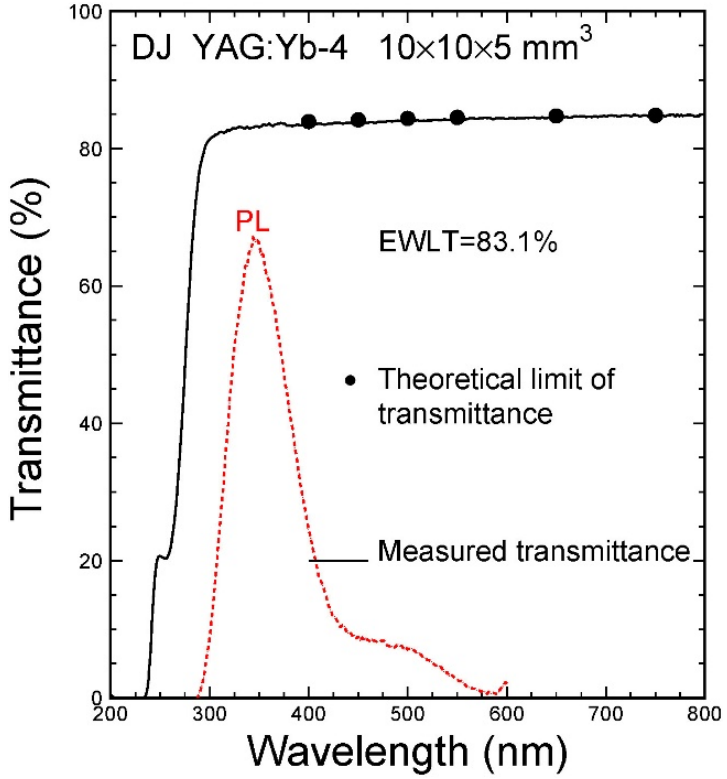

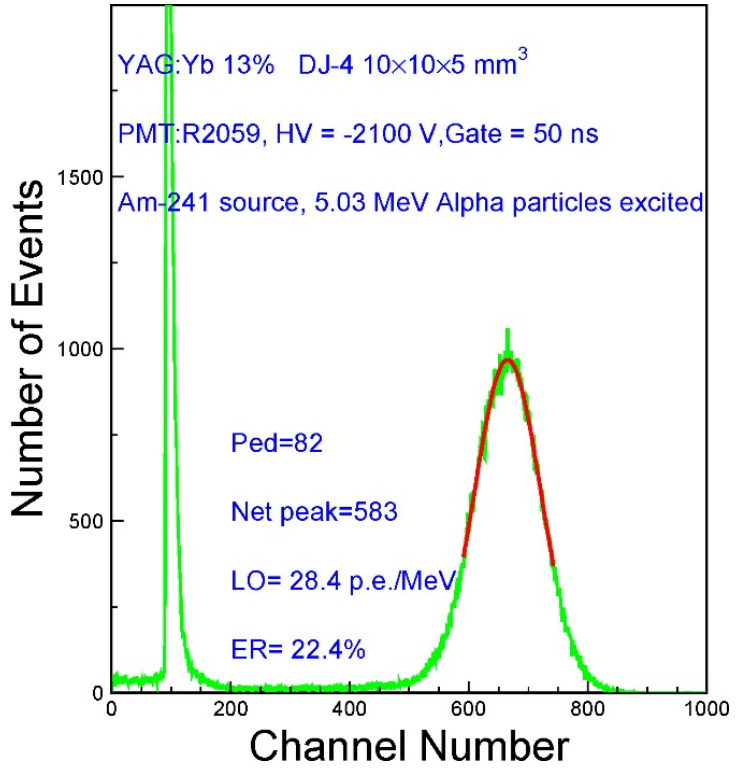

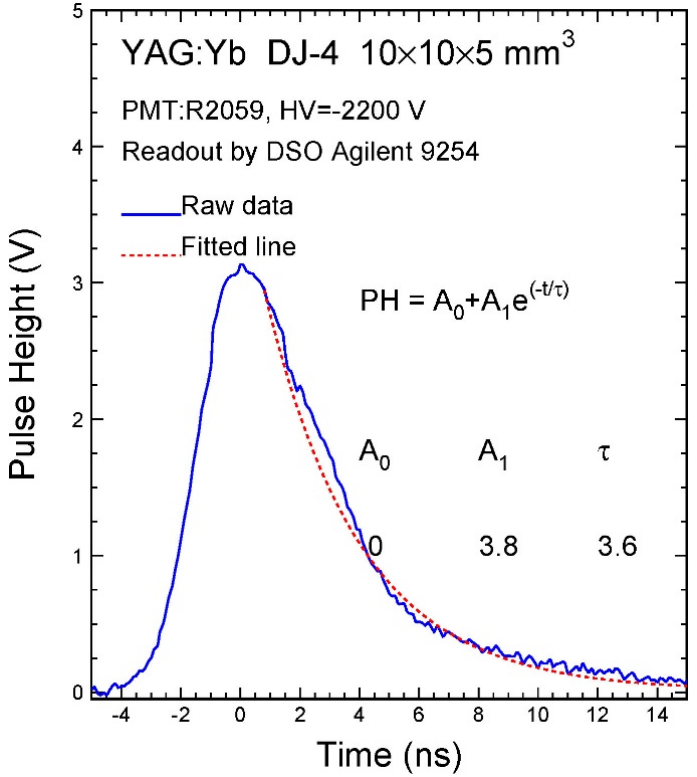

ID	Dimension	EWLT (%)	ER (%)	50 ns LO (p.e./MeV)	Primary Decay Time (ns)
DJ YAG:Yb-4	10×10×5	83.1	22.4	28.4 (α)	3.6

SIC LuAG:Ce-S2 Ceramics

✓ Good LO and ER, and short decay time

× ~ 1 μs slow component

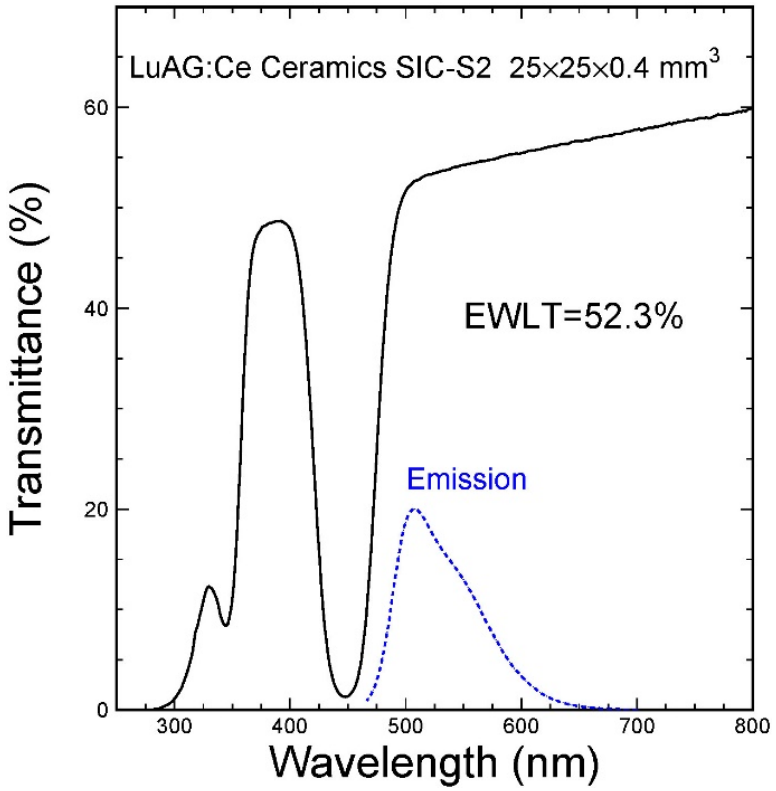

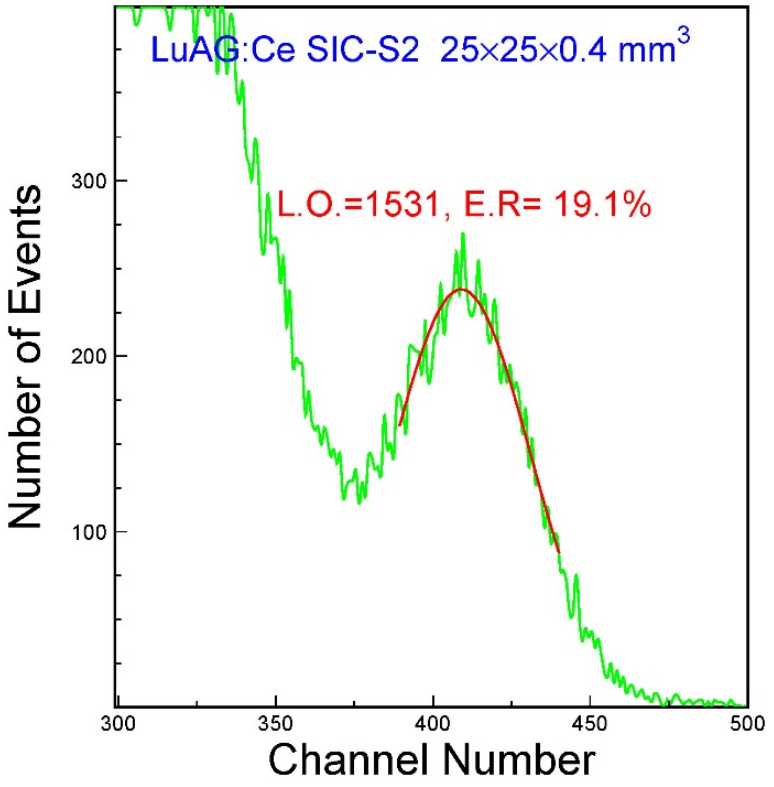

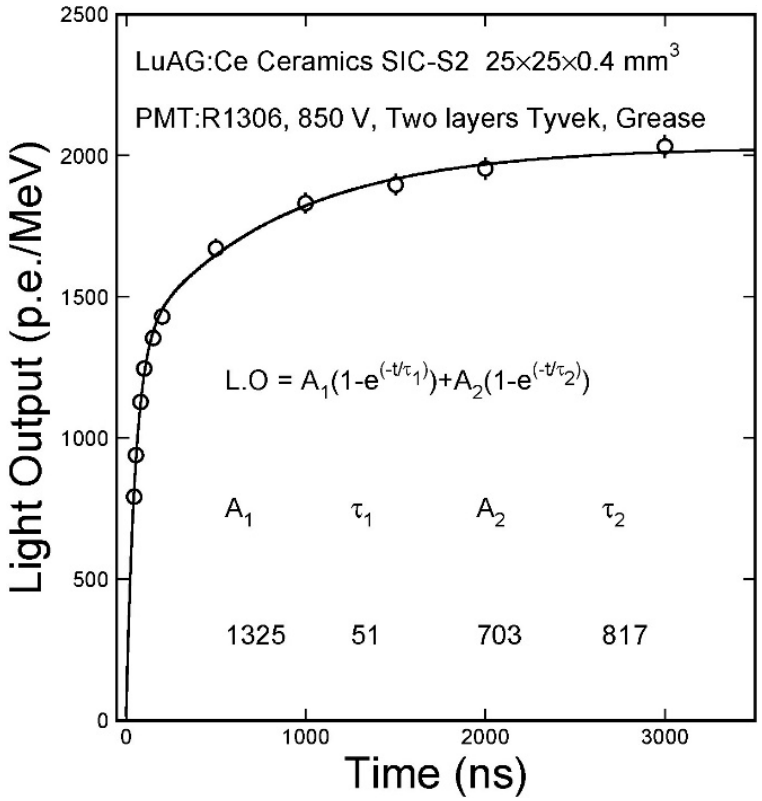

ID	Dimension	EWLT (%)	ER (%)	200 ns LO (p.e./MeV)	Primary Decay Time (ns)
SIC LuAG-S2	25×25×0.4	52.3	19.1	1531	51

Multi-layer Detector Concept

Proc. of SPIE Vol. 9504 95040N

A multilayer high QE photocathode coated thin fast scintillators concept was proposed for GHz hard X-ray imaging:

- Spatial resolution determined layer thickness,
- Overall efficiency defined layer number,
- Maximized conversion of scintillation photon to p.e.,
- Magnetic field extraction of p.e. and image preserving,
- Off-beam p.e. multiplication,
- On-board charge storages.

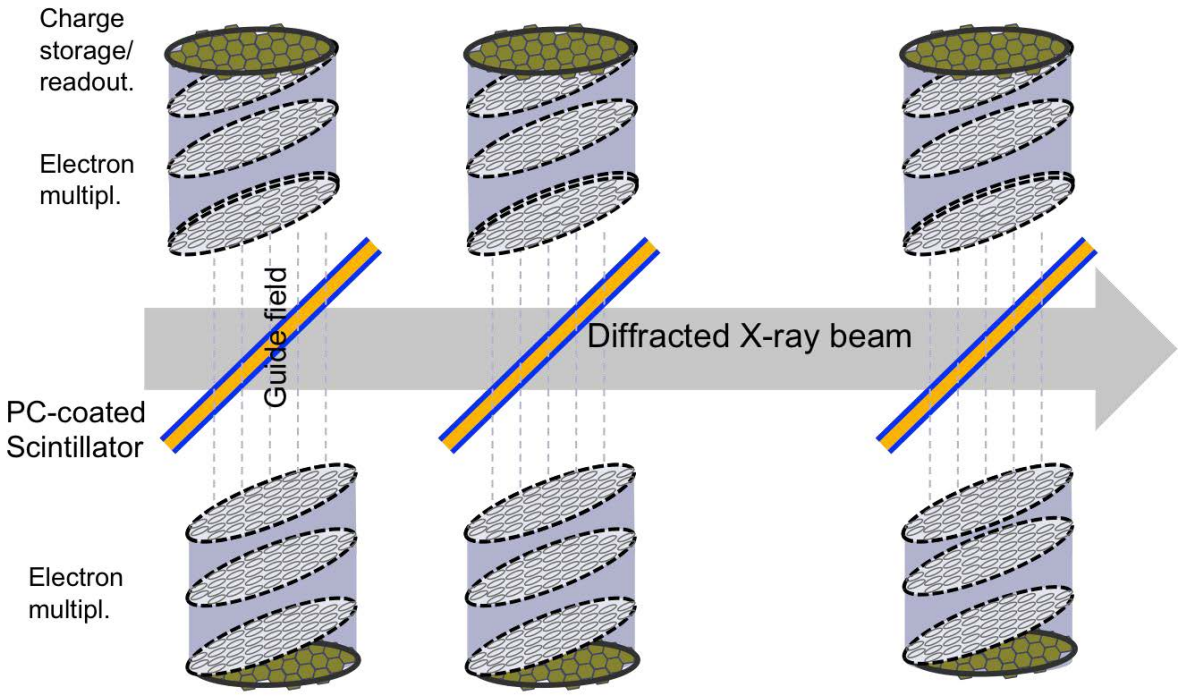

Figure 6. A multi-layer detector architecture for efficient and fast imaging of diffracted X rays. A guide magnetic field perpendicular to the X-ray direction guide the photoelectrons to amplification and storage. The magnetic field also preserves the image contrast due to X-ray absorption at the scintillator location.

Purcell Factor for Ag Particles

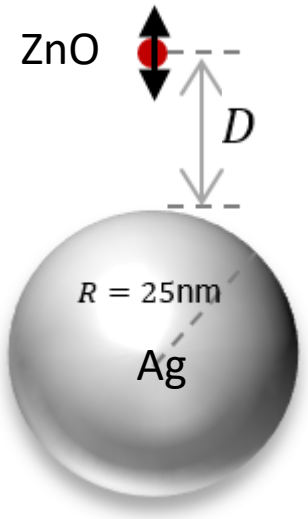

Background PMMA

$\varepsilon_b = 2.17$

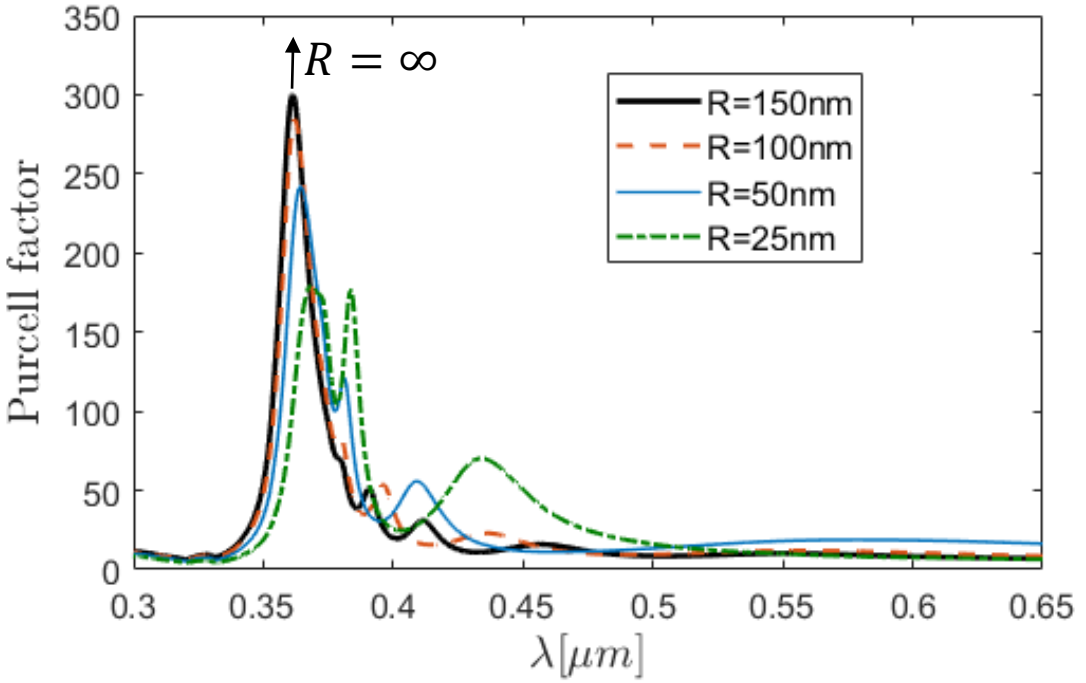

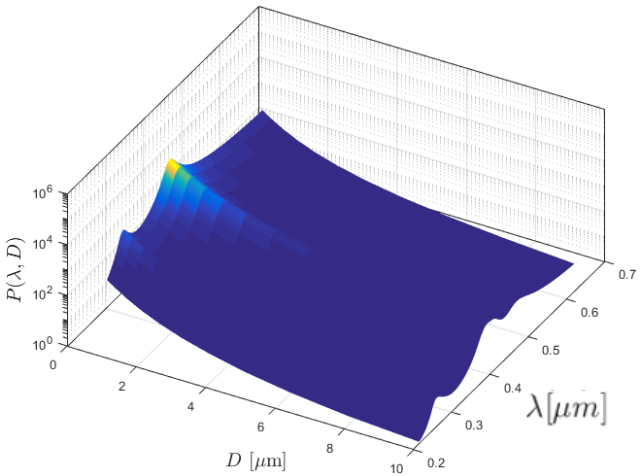

$R = \infty$ is equivalent to a infinite layer. Our simulation is greatly agree with experiments (red circles) as right figure. Agreement includes the peak value, wavelength and bandwidth.

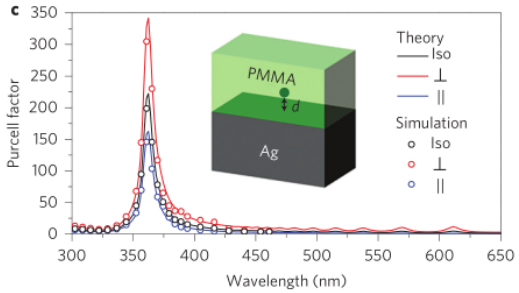

-Lu, Dylan, et al. "Enhancing spontaneous emission rates of molecules using Nano patterned multilayer hyperbolic metamaterials." *Nature nanotechnology*9.1 (2014): 48.

Experimental Proposal

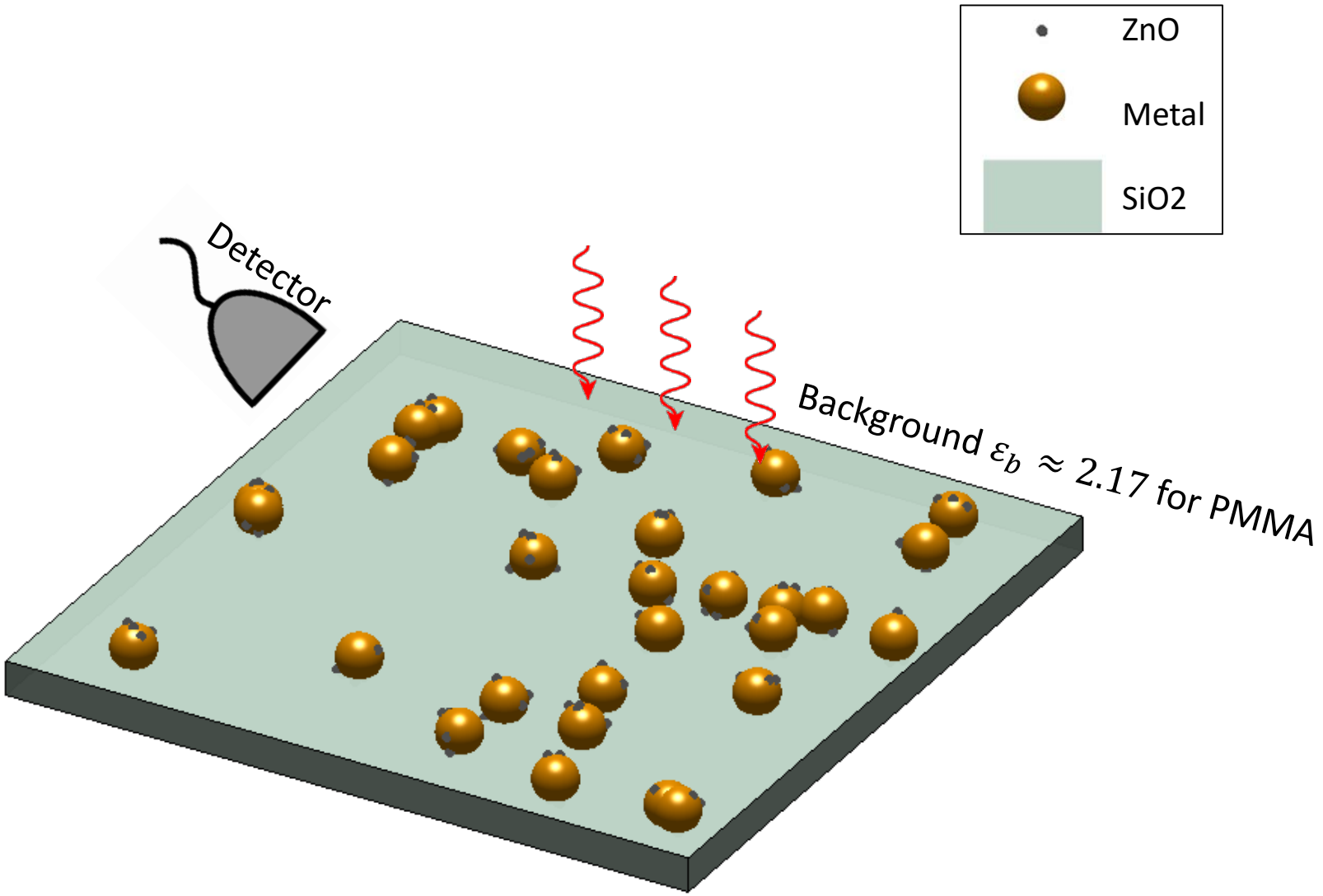

InAs/GaAs QD based Crystal

In recent study[1], *S. Oktyabrsky, et al. report* an ultrafast, no self-absorption, high-efficient room-temperature semiconductor scintillator based on InAs QDs embedded in a GaAs matrix.

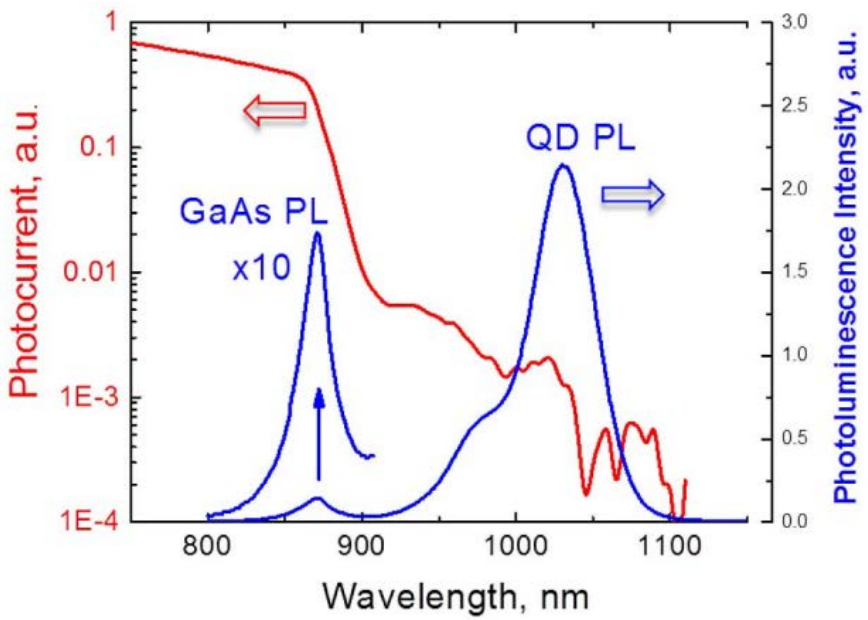

Room temperature photocurrent spectra overlapped with PL spectra of the same QD structure with reduced wetting layer placed in a p-n junction.

Comparison of Some Fast Inorganic Scintillators (source: Scintillator.lbl.gov) With Projected Performance of InAs/GaAs Qd Scintillator

Parameter	BaF_2	LYSO	GaAs/InAs QDs
Density (g/cm^3)	4.89	7.1	5.32
Radiation length, cm	2.03	1.1	2.3
Decay constant, ns	0.8 ns	40	1
Peak emission, nm	195; 220	428	1050
Photon Yield (photons/MeV)	1,400	34,000	240,000
Time between first photons, for 1MeV	0.57ps	1.2 ps	2 fs
Poisson-limited energy resolution at 1MeV (keV) *	62	13	4.8
Radiation hardness, Gy	10^4-10^5	10^4-10^5	$>10^4$
Coupling efficiency	<50%	<50%	~100%

*Assuming collection efficiency = 1

Ref.: [1] S. Oktyabrsky, et al., IEEE Trans. Nucl. Sci. 63, 656 (2016).

$CsPbX_3$ (X=Cl, Br and I) QD

It was reported that nanocrystals of cesium lead halide perovskites ($CsPbX_3$, X = Cl, Br, and I) shows bright emission with a tunable range by quantum size effects.

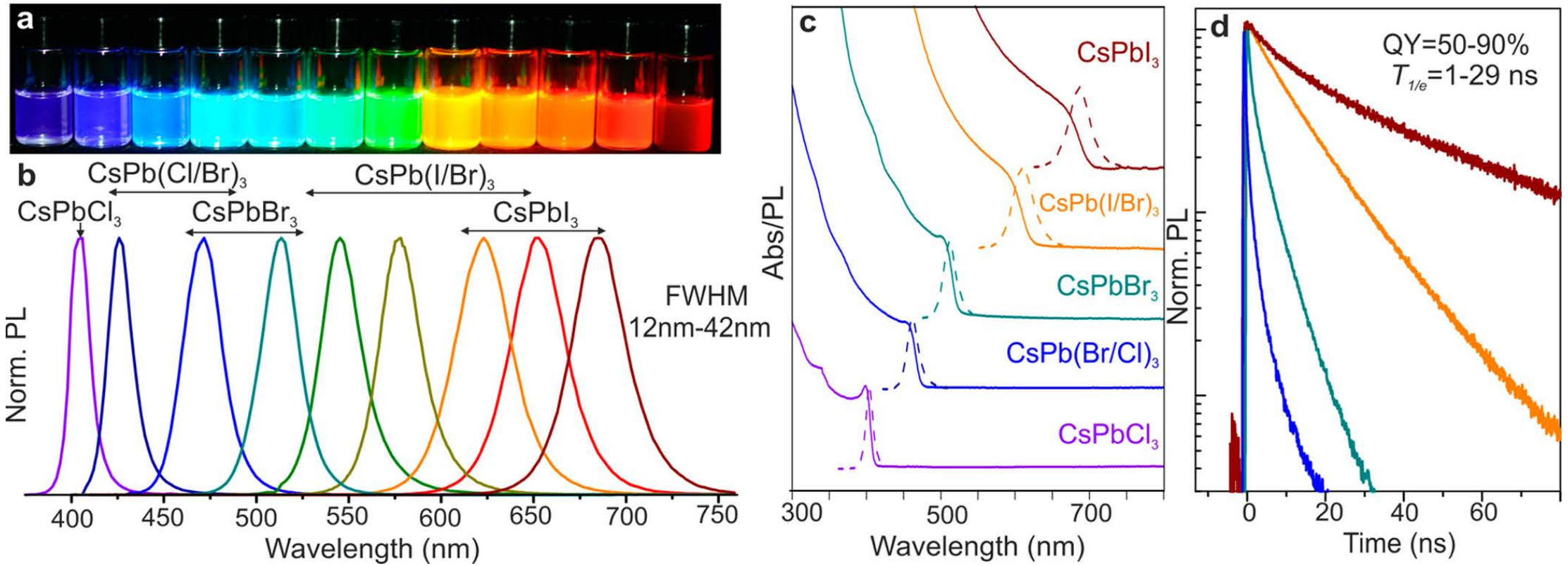

Figure 2. Colloidal perovskite CsPbX3 NCs (X = Cl, Br, I) exhibit size- and composition-tunable bandgap energies covering the entire visible spectral region with narrow and bright emission: (a) colloidal solutions in toluene under UV lamp (λ = 365 nm); (b) representative PL spectra (λexc = 400 nm for all but 350 nm for CsPbCl3 samples); (c) typical optical absorption and PL spectra; (d) time-resolved PL decays for all samples shown in (c) except CsPbCl3.

Nano Lett. 2015, 15, 3692−3696. DOI: 10.1021/nl5048779

Summary

- GHz hard X-ray imaging for the proposed Marie project presents an unprecedented challenge to the speed and radiation hardness of inorganic scintillators.
- BaF_2 crystals provide sufficient fast light with sub-ns decay time and excellent radiation hardness beyond 100 Mrad and 1 x 10^{15} h/cm^2. With its slow component effectively suppressed by yttrium doping BaF_2:Y promises a fast and robust front imager.
- Bulk ZnO:Ga crystals suffer from serious self-absorption. Enhanced UV emission in Ag/Au ZnO core-shell nano particles hints a thin film based approach.
- Our plan is to investigate along both lines: BaF_2:Y crystals, and ZnO QD/NP based thin film for the Marie project with a close collaboration between the NP, HEP and material science communities.

Acknowledgements: DOE Award DE-SC001192

Purcell effect for enhancing ZnO luminescence (Theoretical framework)

Hybrid system as experimental frame

Total field :

$$\underbrace{\langle \hat{\boldsymbol{E}}_{\boldsymbol{m}}(\boldsymbol{r})\rangle}_{(a)} = \underbrace{\boldsymbol{E}_m^L(\boldsymbol{r})}_{(b)} + \underbrace{\frac{\omega^2}{\epsilon_0 c^2}\overleftrightarrow{\boldsymbol{G}}(\boldsymbol{r},\boldsymbol{r}_0;\omega)\cdot\boldsymbol{\mu}\langle S\rangle}_{(c)}$$

Dipole moment: $\langle \hat{S}\rangle = \frac{-\Omega[2\Delta - i\gamma_m]}{4\Delta^2+2|\Omega|^2+\gamma_m^2}$

Rabi frequency: $\Omega = 2\boldsymbol{\mu}\cdot\boldsymbol{E}_m^L(\boldsymbol{r}_0)$

Δ is detuning

$\overleftrightarrow{\boldsymbol{G}}(\boldsymbol{r},\boldsymbol{r}_0;\omega)$ is Dyadic Green's function

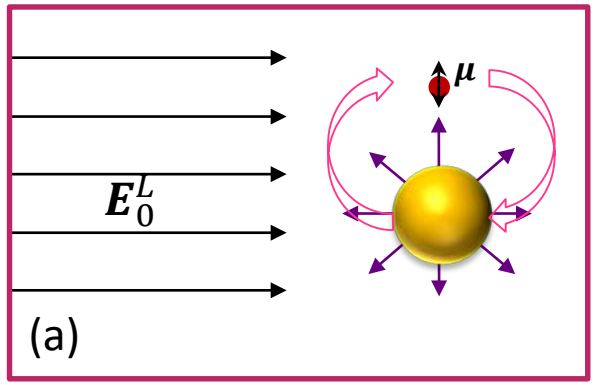

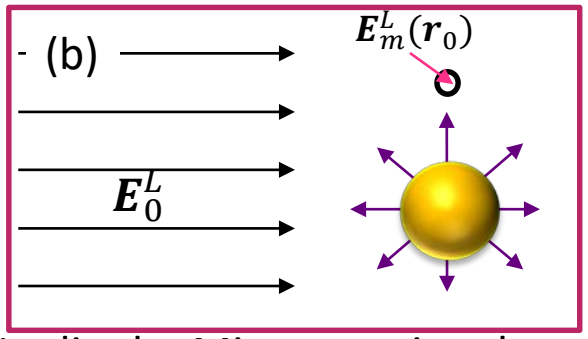

No dipole: Mie scattering theory

NOTE: dipole is considered as a point in theory. In experiment, ZnO is the dipole.

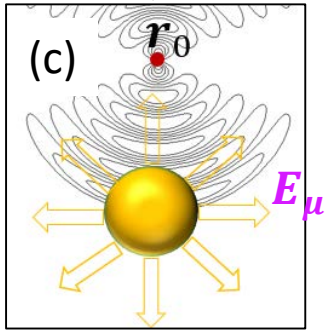

Dipole vs. Nanostructure: dyadic Green's function

In numerical calculation, the dyadic Green's function is the kernel.

$$\gamma_m = 2\mathrm{Im}[\boldsymbol{\mu}\cdot\boldsymbol{E}_{\boldsymbol{\mu}}(\boldsymbol{r}_0)] = 2Im[\boldsymbol{\mu}\cdot\overleftrightarrow{\boldsymbol{G}}(\boldsymbol{r},\boldsymbol{r}_0;\omega)\cdot\boldsymbol{\mu}]$$

γ_m/γ_0 is Purcell enhancement factor

Purcell Factor for Ag Particles

Particle size: R=20nm

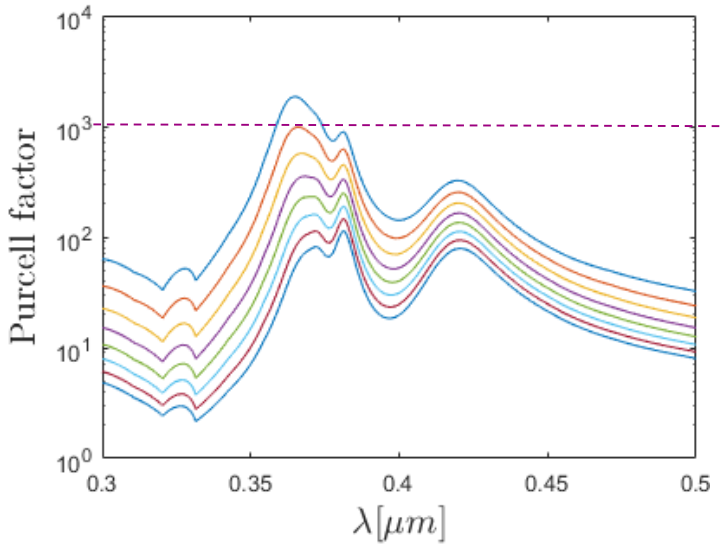

Particle size: R=50nm

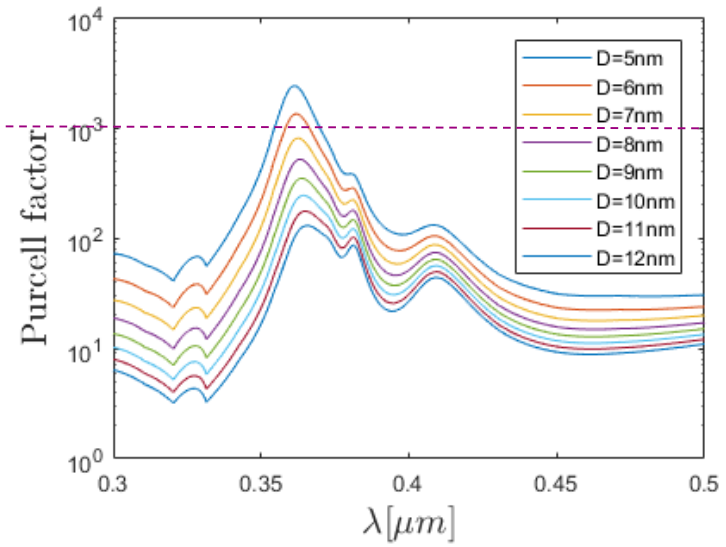

- The Purcell factor is sensitive to the distance between ZnO and metallic nanoparticle.
- The bandwidth of Purcell factor is stable for variety of distance D.

The spatial resolution Vs thickness of thin scintillator

Z. Wang et al. has proposed the following equation to determine the maximum thickness of scintillator for a scintillator camera:

$$R_{spatial} = 2dsin\theta_c = 2dsin\frac{1}{n}$$

where $R_{spatial}$ is the spatial resolution, d is the thickness of scintillator, θc is the n is the reflective index of scintillator at emission peak.

- **The spatial resolution ($R_{spatial}$) of a scintillator camera is limited by the scintillator thickness (d); For an air-to-scintillator interface, the total internal reflection angle (θ_c) is *asin(1/n)* for a flat interface;**
- **$R_{spatial}$ is limited to $2dsin\theta_c$ for a thickness *d*, assuming the light interacts with the interface only once (~ 95% of the light for incidental angles less than the Brewster's angle of *atan(1/n)*). For 100-μm spatial resolution, the thickness of BaF_2 crystal with a reflective index of 1.54 @220nm cannot exceed 71μm.**

The maximum thickness of thin scintillator determined by X-ray imaging spatial resolution

	LYSO:Ce	LSO:Ce,Ca	BaF_2	CsF	$CeBr_3$	$LaBr_3$:Ce	YAG:Yb	YAP:Yb	ZnO:Ga	PbI_2	GaAs/In As QDs	Plastic scintillator (BC 404)
Reflective index at emission peak (n)	1.82	1.82	1.54	1.49	1.9	1.9	1.87	1.96	2.1	3.4	3.47	1.58
1/n	0.549	0.549	0.649	0.671	0.526	0.526	0.535	0.510	0.476	0.294	0.288	0.633
atan(1/n)	0.502	0.502	0.576	0.591	0.484	0.484	0.491	0.472	0.444	0.286	0.281	0.564
Maximum thickness (d)for 100um spatial resolution (mm)	86	86	71	68	90	90	89	93	101	167	171	73

Ref.: Z. Wang, C. W. Barnes, J. S. Kapustinsky, C. L. Morris, R. O. Nelson, F. Yang, L. Zhang, and R.-Y. Zhu, *Proc. of SPIE 2015*, pp. 95040N.